Check for updates

The functional characterization of *LjNRT2.4* indicates a novel, positive role of nitrate for an efficient nodule N_2-fixation activity

Vladimir Totev Valkov, Stefano Sol, Alessandra Rogato and Maurizio Chiurazzi

Institute of Biosciences and Bioresources, IBBR, CNR, Via P. Castellino 111, Napoli 80131, Italy

Author for correspondence:
Maurizio Chiurazzi
Tel: +39 081 6132433
Email: maurizio.chiurazzi@ibbr.cnr.it

Received: *11 March 2020*
Accepted: *27 May 2020*

New Phytologist (2020) **228:** 682–696
doi: 10.1111/nph.16728

Key words: hypoxia, nitrate, nitric oxide (NO), nodules, NRT2, symbiotic N_2 fixation.

Summary

- Atmospheric nitrogen (N_2)-fixing nodules are formed on the roots of legume plants as result of the symbiotic interaction with rhizobia. Nodule functioning requires high amounts of carbon and energy, and therefore legumes have developed finely tuned mechanisms to cope with changing external environmental conditions, including nutrient availability and flooding. The investigation of the role of nitrate as regulator of the symbiotic N_2 fixation has been limited to the inhibitory effects exerted by high external concentrations on nodule formation, development and functioning.
- We describe a nitrate-dependent route acting at low external concentrations that become crucial in hydroponic conditions to ensure an efficient nodule functionality. Combined genetic, biochemical and molecular studies are used to unravel the novel function of the *LjNRT2.4* gene.
- Two independent null mutants are affected by the nitrate content of nodules, consistent with *LjNRT2.4* temporal and spatial profiles of expression. The reduced nodular nitrate content is associated to a strong reduction of nitrogenase activity and a severe N-starvation phenotype observed under hydroponic conditions. We also report the effects of the mutations on the nodular nitric oxide (NO) production and content.
- We discuss the involvement of LjNRT2.4 in a nitrate-NO respiratory chain taking place in the N_2-fixing nodules.

Introduction

Nitrate and ammonium are the two main sources of nitrogen (N) controlling plant growth and development. Plants have evolved a complex molecular network to sense the external and endogenous N status in order to efficiently satisfy rapidly changing demands. Nitrogen sensing may involve proteins involved in N-uptake, such as transceptors of nitrate or ammonia (Ho *et al.*, 2009; Rogato *et al.*, 2010), or sensors of internal N-status (Gutierrez *et al.*, 2008; Swift *et al.*, 2019). In the case of nitrate, a primary role in the networks governing nitrate assimilation, storage and distribution among different plant tissues and organs, is played by two protein families – the low-affinity Nitrate Transporter Peptide (NPF) and the high-affinity Nitrate Transporter (NRT2; Wang *et al.*, 2018). NPF is a large family of 53, 80 and 86 members in *Arabidopsis thaliana*, *Oryza sativa* and *Lotus japonicus*, respectively (Tsay *et al.*, 2007; Léran *et al.*, 2014; Sol *et al.*, 2019). The NPF members are divided into eight subfamilies and able to transport different substrates (Léran *et al.*, 2014). NRT2 proteins form small families of plant transporters in plants including seven, four and four members in *A. thaliana*, *O. sativa* and *L. japonicus*, respectively (Glass *et al.*, 2001; Cai *et al.*, 2008; Criscuolo *et al.*, 2012). By contrast to NPF proteins, all of the NRT2 proteins characterized thus far in higher plants transport only nitrate, displaying a high-affinity activity with the exceptions of the *Lycopersicon esculentum* LeNRT2.3 that shows a low-affinity nitrate uptake activity in *Xenopus* oocytes (Fu *et al.*, 2015) and the *O. sativa* NRT2.4 that was reported to behave as a dual-affinity nitrate transporter in *Xenopus* (Wei *et al.*, 2018). NRT2 proteins are proton-coupled transporters and four of seven NRT2 genes found in *Arabidopsis* show a nitrate-related phenotype when mutated (Chopin *et al.*, 2007; Kiba *et al.*, 2012; Wang *et al.*, 2018). In particular, AtNRT2.1; 2.2; 2.4 and 2.5 are involved in nitrate uptake into the root system, where these genes display different spatial profiles of expression (Kiba *et al.*, 2012; Lezhneva *et al.*, 2014). Recently, a post-transcriptional regulation through a phosphorylation reaction, which increases the stability of the protein under nitrate-limited conditions, has been reported for AtNRT2.1 (X. Zou *et al.*, 2019). *AtNRT2.4* and *ATNRT2.5* also are expressed in the phloem tissue where they play a role on nitrate loading and mobilization to the shoot under conditions of N starvation (Kiba *et al.*, 2012; Lezhneva *et al.*, 2014). A similar function was reported for OsNRT2.3a that is expressed in the xylem parenchima of rice roots (Tang *et al.*, 2012). NRT2s are not functional alone, as an additional component called NAR2/NRT3, that interacts physically with NRT2s, is normally required for plasma membrane targeting and NRT2 stability (Kotur *et al.*, 2012). The exceptions are represented by AtNRT2.7 and OsNRT2.4 that achieve nitrate uptake in *Xenopus* alone, without NAR2 co-expression (Chopin *et al.*,

© 2020 The Authors
New Phytologist © 2020 New Phytologist Trust

14698137, 2020, 2, Downloaded from https://nph.onlinelibrary.wiley.com/doi/10.1111/nph.16728 by CNR GROUP II Istituto di Scienza dell, Wiley Online Library on [23/05/2024]. See the Terms and Conditions (https://onlinelibrary.wiley.com/terms-and-conditions) on Wiley Online Library for rules of use; OA articles are governed by the applicable Creative Commons License

2007; Wei *et al.*, 2018). AtNRT2.7 shows a peculiar vacuolar membrane subcellular localization and is involved on nitrate accumulation in the seeds (Chopin *et al.*, 2007), whereas OsNRT2.4 is required for nitrate-regulated root and shoot growth (Wei *et al.*, 2018).

The biological N_2-fixation (BNF) which evolved in legume plants represents an objective advantage owing to the capacity of converting atmospheric N_2 into plant-assimilable NH_3. However, both formation and functioning of N_2-fixing nodules require high amounts of carbon and energy, and, therefore, it is not surprising that legumes have developed finely tuned mechanisms to regulate nodule formation, development and functioning in relation to the N demand of the plants. In particular, when a N source is available in the rhizosphere, nodule formation capacity declines as well as the efficiency of existing N_2-fixing nodules (Carroll & Gresshoff, 1983; Fujikake *et al.*, 2003; Barbulova *et al.*, 2007; Omrane & Chiurazzi, 2009; Naudin *et al.*, 2011; Cabeza *et al.*, 2014). In the case of nodule functioning, the short exposure of nodulated roots to 5 mM nitrate strongly inhibits N_2-fixation activity and this response is quickly reversed once nitrate is removed (Cabeza *et al.*, 2014). Different hypotheses have been developed to explain such a strong impact of high nitrate on nodule functioning: (1) reduction of oxygen permeability (Minchin *et al.*, 1986; Vessey *et al.*, 1988), (2) competition of the nitrate reduction activity as sink for assimilates and energy (Vessey & waterer, 1992; Fujikake *et al.*, 2003) and (3) nitrate-mediated effect on the shoot allocation of photosytate products (Fujikake *et al.*, 2003). Very recently, the involvement of NIN-like transcription factors on the nitrate-mediated nitrogenase activity inhibitory pathway has been reported in *L. japonicus* and *Medicago truncatula* (Nishida *et al.*, 2018; Lin *et al.*, 2018) that could play a role in the significant transcriptional regulation observed after the nodule nitrate treatment (Cabeza *et al.*, 2014; Schulze *et al.*, 2020). N_2-fixing invaded cells are filled with organelles called symbiosomes that are the result of an endocytosis process enclosing invading bacteria in a plant-derived membrane, the peri-bacteroidal membrane (PBM). Inside the symbiosome, bacteria stop dividing and differentiate into the N_2-fixing bacteroids. N_2-fixation occurs via the action of the nitrogenase enzyme through an energy-intensive process requiring O_2 for respiration to generate ATP and reducing equivalents for reduction of N_2 to NH_3. A finely tuned mechanism is active in the N_2-fixing cells to ensure a correct balance between the microaerophilic condition that must be maintained to avoid nitrogenase inactivation, and the high rates of respiration in mitochondria and bacteroids of invaded cells (Bergensen, 1996; Witty & Minchin, 1998). To satisfy these conflicting demands, a crucial role is played by the high-affinity O_2^- binding protein leghemoglobin (Lb), which is present at millimolar concentrations in the N_2-fixing cells, allowing the delivery of O_2 efficiently to mitochondria and bacteroids for respiration while buffering free O_2 at the required level (Appleby, 1984). Furthermore, a nitrate–NO respiration pathway that provides an alternative electron transfer chain has been also reported in *M. truncatula* nodules under normoxic conditions, which becomes particularly important under hypoxia conditions to support the energy status required for efficient N_2-fixation (Horchani *et al.*, 2011). Consistently, hypoxia or flooding conditions trigger NO accumulation in *M. truncatula* and soybean nodules (Sanchez *et al.*, 2010; Horchani *et al.*, 2011).

The metabolic pathways of functioning nodules strictly aimed to ensure an efficient N_2-fixation process, are mirrored by specific gene expression profiles for related metabolic enzymes. Several transcriptomic analyses allowed the classification of genes induced in N_2-fixing nodules that encode a significant percentage of transporter proteins (Colebatch *et al.*, 2004; Hogslund *et al.*, 2009; Takanashi *et al.*, 2012). NPF and NRT2 proteins are largely represented among this category of nodule-induced transporter genes (Criscuolo *et al.*, 2012; Valkov & Chiurazzi, 2014; Clarke *et al.*, 2015). However, at the moment the involvement of nitrate transporters on the regulation of the nodulation process has been reported only for *MtNPF1.7* controlling the nodule meristem formation and invasion (Teillet *et al.*, 2008; Yendrek *et al.*, 2010) and *LjNPF8.6* that plays a role in the regulation of nodule functioning (Valkov *et al.*, 2017).

We report here the functional characterization of a member of the *L. japonicus* NRT2 family involved in the control of nodular nitrate content that indicates a critical role for this pathway on the efficient functioning of N_2-fixing nodules.

Materials and Methods

Plant material and growth conditions

All experiments were carried out with *Lotus japonicus* ecotype B-129 F12 GIFU (Handberg & Stougaard, 1992; Jiang & Gresshoff, 1997). Plants were cultivated in a controlled growth chamber with a light intensity of 200 μmol m^{-2} s^{-1} at 23°C with a 16 h : 8 h, light : dark cycle. Seed sterilization was performed as described in Barbulova *et al.* (2005). Five days after sowing in axenic conditions on H_2O agar Petri dishes, unsynchronized seedlings were discarded. *Mesorhizobium loti* inoculation was performed at 7 d after sowing as described in Barbulova *et al.* (2005). The strain R7A used for the inoculation experiments is grown in liquid TYR-medium supplemented with rifampicin (20 mg l^{-1}).

Three different plant growth conditions were used in the described experiments. For those shown in Figs 2, 3, 6 and 7, 5 d after sowing, seedlings were transferred in Petri dish axenic conditions, on solid growth media with the same composition as Gamborg B5 medium (Gamborg, 1970), except that $(NH_4)_2SO_4$ and KNO_3 were omitted and substituted by the proper N source at the required concentration. KCl was added, when necessary to the medium to replace the same concentrations of potassium source. The media containing vitamins (G0415; Duchefa) were buffered with 2.5 mM 2-(*N*-morpholino)ethanesulfonic acid (MES, M1503.0250; Duchefa) and pH-adjusted to 5.7 with KOH. After germination, unsynchronized seedlings were discarded.

For the experiments shown in Figs 8 and 9, the same procedure described above was followed for germination and inoculation, except that at 4 d post-inoculation (9 d after sowing), plants were transferred into hydroponic cultures, with the same B5-derived medium used for axenic conditions. The pH of the

© 2020 The Authors
New Phytologist © 2020 New Phytologist Trust

14698137, 2020, 2, Downloaded from https://nph.onlinelibrary.wiley.com/doi/10.1111/nph.16728 by CNR GROUP II Istituto di Scienza dell', Wiley Online Library on [23/05/2024]. See the Terms and Conditions (https://onlinelibrary.wiley.com/terms-and-conditions) on Wiley Online Library for rules of use; OA articles are governed by the applicable Creative Commons License

nutrient solution was monitored every 4 d and KNO_3 was re-supplied every 5 d at the required concentrations. Roots were completely submerged and the level of the solution was maintained daily if needed. Moderate stirring was applied every 2 d to the medium to ensure homogenous distribution.

For the experiment shown in Fig. 9(a), plants grown in normoxic conditions (N), were transferred at 4 d post-inoculation into pots with clay granules (leca). Plants were watered every 5 d with the same B5-derived solution.

Estimation of anthocyanin

Stem tissue from three plants per assay was weighed and then extracted with 99 : 1 methanol : HCl (v/v) at 4°C. The OD_{530} and OD_{657} for each sample were measured and relative anthocyanin concentrations determined with the equation $OD_{530} - (0.25 \times OD_{657}) \times$ extraction volume (ml) × 1/FW of tissue sample (g) = relative units of anthocyanin/g FW tissue.

Determination of Acetylene-Reduction Activity (ARA)

The ARA assay has been described in D'Apuzzo *et al.* (2015) and Garcìa-Calderon *et al.* (2012). Detached roots with comparable number of nodules were placed in 10-ml glass vials and sealed with parafilm. The vials were injected with 1 ml acetylene (C_2H_2 : air = 1 : 9 v/v) by using an autosampler syringe. After 30 min of incubation at 25°C, 1 ml of sample was collected and injected through the septa of the gas chromatograph (Clarus 580; PerkinElmer, Beaconsfield, UK) and the area of the obtained peak of ethylene measured. After the analysis, the nodules were detached from the root samples under the microscope to carefully isolate these from the root material and weighed collectively. The acetylene reduction activity of the nodules was calculated as the amount of ethylene produced per time and mass of nodules (μmols × 1/h × 1/g nod) by using the following formula: ethylene area × nodule weight $(g)^{-1} \times t(h)^{-1} \times 4.12/8880\,000$, where 4.12 is the μmols of ethylene in 1 ml of gas mixture kept at 1 atm at 20°C.

Determination of nitrate content

Detached nodules were first weighed and then frozen at −80°C. Crude extracts were prepared by grinding the frozen samples with a tissue lyser (85220; Qiagen) at 29 Hz for 1 min 30 s. The powder was immediately resuspended in H_2O (6 ml $H_2O\ g^{-1}$ FW), vortexed and centrifuged at 16.2 ***g*** to recover the supernatant. The colorimetric determination of nitrate content in leaves and roots extracts followed the procedure described by Pajuelo *et al.* (2002). 200 μl of 5% (w/v) salicylic acid in concentrated H_2SO_4 was added to 50-μl aliquots from the crude extracts and left to react for 20 min at room temperature. NaOH (4.75 ml of 2 N) was added to the reaction mixtures and the absorbance at 405 nm scored after cooling. A calibration curve of known amounts of $NaNO_3$ (74246; Sigma) dissolved in the standard extraction buffer was used for analytical determinations. Controls were set up without salicylic acid.

NO production assay

We used the procedure described in Horchani *et al.* (2011) using the following detection medium: 10 mM tris-HCl, pH 7.5, 10 mM KCl, in the presence of 10 μM DAF-2 (D23844; Thermofisher, Waltham, MA, USA). First 15–30 mg of detached nodules (normally from two to three plants) were incubated in the dark at 23°C in 1.5-ml Eppendorf tubes containing 500 μl of detection medium with the fluorescent probe DAF-2 (10 μl). Different pO_2 in the incubation medium were obtained with a permanent bubbling of either ambient air (21% O_2; normoxic conditions) or a 1% : 99% oxygen : N_2 (v/v; 1% O_2; hypoxic conditions) gas stream. The 1% oxygen value for hypoxic conditions was based on the pO_2 data reported in waterlogged soils by Gibbs & Greenway (2003). The NO released into the detection medium was analyzed by taking aliquots at various times and measuring at the Jasco spectrofluorimeter FP-8200 (Jasco Europe Srl, Cremella, Italy), the fluorescence of DAF-2T, the reaction product from DAF-2 and NO. Excitation was 495 nm and emission 515 nm fluorescence. In these conditions, NO release was found to be linear from 30 min to ≥4 h incubation time. Blank samples contained detection buffer with DAF-2 without nodules.

NO content assay

Fifteen to thirty milligram of detached nodules (normally from two to three plants) were ground with a tissue lyser (85,220; Qiagen) at 29 Hz for 1 min 30 s. The powder was immediately resuspended in 500 μl of detection medium with 10 μM DAF-2 probe and centrifuged at 4°C for 10 min. The fluorescence of the supernatant was measured at the spectrofluorimeter (excitation 495 nm; emission 515 nm).

Lotus japonicus transformation procedures

Binary vectors were conjugated into the *Agrobacterium rhizogenes* 15834 strain (Stougaard *et al.*, 1987). *A. rhizogenes*-mediated *L. japonicus* transformations were performed as described in Bastianelli *et al.* (2009) and inoculation of composite plants was asdescribed in Santi *et al.* (2003).

Protoplast transformation

Leaf protoplasts were prepared and transformed according to Pedrazzini *et al.* (1997), using 3-wk-old *N. tabacum* plants. DNA (40 μg of each construct) was introduced into 1×10^6 protoplasts by polyethylene glycol (PEG)-mediated transfection. After 16 h incubation in the dark at 25°C, yellow fluorescent protein (YFP) fluorescence in protoplast cells was detected by confocal microscopy.

Plasmid preparation

pr*LjNRT2.4-gus*A: the PCR-amplified fragment containing 1038 bp upstream of the ATG was obtained on genomic DNA with forward and reverse oligonucleotides containing *Sal*I and

© 2020 The Authors
New Phytologist © 2020 New Phytologist Trust

14698137, 2020, 2, Downloaded from https://nph.onlinelibrary.wiley.com/doi/10.1111/nph.16728 by CNR GROUP II Istituto di Scienza dell', Wiley Online Library on [23/05/2024]. See the Terms and Conditions (https://onlinelibrary.wiley.com/terms-and-conditions) on Wiley Online Library for rules of use; OA articles are governed by the applicable Creative Commons License

*Bam*HI sites, respectively (Supporting Information Table S1). The amplicon was subcloned as *Sal*I–*Bam*HI fragment into the pBI101.1 vector (Jefferson, 1987) to obtain the T-DNA construct. Finally, the pr*LjNRT2.4-gus*A cassette was subcloned as an *Eco*RI–*Hin*dIII fragment into the pIV10 plasmid for co-integration into the pAR1193 (Stougaard *et al.*, 1987).

LjNRT2.4-YFP: the PCR-amplified fragment obtained on nodular cDNA with forward and reverse oligonucleotides containing *Bam*HI and *Xho*I sites, respectively (Table S1), was subcloned as *Bam*HI–*Xho*I fragment into the pENTR™1A plasmid (A10462; ThermoFisher). The resulting donor plasmid was mixed with the pEarleyGate 104 destination vector to obtain the YPF-LjNRT2.4 fusion (Earley *et al.*, 2006).

Quantitative real-time (qRT)-PCR

Real-time PCR was performed with a DNA Engine Opticon 2 System, MJ Research (Waltham, MA, USA) using SYBR to monitor dsDNA synthesis. The procedure is described in Ferraioli *et al.* (2004). The ubiquitin (*UBI*) gene (AW719589) was used as an internal standard. The oligonucleotides used for the qRT-PCR are listed in Table S1.

LORE1 lines analyses

LORE1 lines 30061917 and 30083188 were obtained from the *LORE1* collection (Fukai *et al.*, 2012; Urbanski *et al.*, 2012; Malolepszy *et al.*, 2016). Plants in the segregating populations were genotyped and expression of homozygous plants tested with oligonucleotides listed in the Table S1. After PCR genotyping, shoot cuts of the homozygous plants were cultured in axenic conditions and root induction obtained through a 7 d exposure to 0.1 mg l^{-1} naphthaleneacetic acid (NAA, Duchefa cat. G0903; Duchefa Biochemie, Haarlem, Netherlands).

Histochemical glucuronidase (GUS) and *lacZ* analyses

Histochemical GUS and *lacZ* staining were performed as described by Rogato *et al.* (2008, 2016) and Omrane *et al.* (2009), respectively.

Confocal imaging

Confocal microscope analyses were performed using a LeicaDMi8 (Leica Biosystems, Wetzlar, Germany) laser scanning confocal imaging system. For YFP detection, excitation was at 488 nm, and detection between 515 and 530 nm. For the chlorophyll detection, excitation was at 488 nm and detection over 570 nm.

Phylogenetic studies

The evolutionary history was inferred using the Neighbor-Joining method (Saitou & Nei, 1987). The percentage of replicate trees in which the associated taxa clustered together in the bootstrap test (500 replicates) are shown next to the branches (Felsenstein, 1985). The evolutionary distances were computed using the JTT matrix-based method (Jones *et al.*, 1992) and are in the units of the number of amino acid substitutions per site. The analysis involved 49 amino acid sequences. All positions with < 65% site coverage were eliminated. That is, < 35% alignment gaps, missing data, and ambiguous bases were allowed at any position. There were a total of 501 positions in the final dataset. Evolutionary analyses were conducted in MEGA7 (Kumar *et al.*, 2016).

Statistical analyses

Statistical analyses were performed using the VASSARSTATS two-way factorial ANOVA for independent samples program (http://vassarstats.net/).

Results

LjNRT2.4 identifies a peculiar member of the plant NRT2 families

The *L. japonicus* NRT2 family has been described and preliminarily characterized by Criscuolo *et al.* (2012). Four members were identified including two paralogues located on chromosome 3, sharing 95% of nucleotide identity, named *LjNRT2.1* and *LjNRT2.2*. We have now assigned the names *LjNRT2.3* and *LjNRT2.4* to the two members located on chromosomes 4 and 1, respectively (Table S2). *LjNRT2.4* (Lj1g3v3646440.1 in the genomic assembly build 3.0; http://www.kazusa.or.jp/lotus/index.html) encodes for a 460 amino acid protein with 12 transmembrane predicted domains (Fig. S1; Tusnády & Simon, 2001) and a predicted molecular mass of 49.16 kDa. When the LjNRT2.4 sequence was used as query against the *A. thaliana* NRT2 family the highest value of amino acid identity was shared with AtNRT2.7 (63%; Table S2). AtNRT2.7 is the most diverged of all the NRT2 sequences (Plett *et al.*, 2010) and holds a unique biochemical feature among the AtNRT2 transporters, being the only member that does not interact physically with AtNAR2, a partner protein required to enhance nitrate uptake in *Xenopus laevis* oocytes (Kotur *et al.*, 2012). More recently, the lack of NAR2 requirement also has been reported for the OsNRT2.4 protein (Wei *et al.*, 2018). Interestingly, the AtNRT2.7 highly conserved sequences could be identified only in some of the genomes analyzed, indicating a divergent evolution of this gene (Fig. 1). The phylogenetic tree shown in Fig. 1, based on the alignment of nine plant NRT2 protein families, highlighted the close relationship of a small subgroup of AtNRT2.7 horthologues identified in the genomes of *A. thaliana, O. sativa, Zea mays, L. japonicus, Arachis hypogaea* and *Cyrysanthemum morifolium*, and absent in *Hordeum vulgare, Glycine max* and *M. truncatula*.

LjNRT2.4 is expressed in root and nodule vascular tissues and the protein localizes at the plasma membrane

A preliminary analysis of the regulatory profile of expression of the gene *LjNRT2.4* has been reported in Criscuolo *et al.* (2012)

© 2020 The Authors
New Phytologist © 2020 New Phytologist Trust

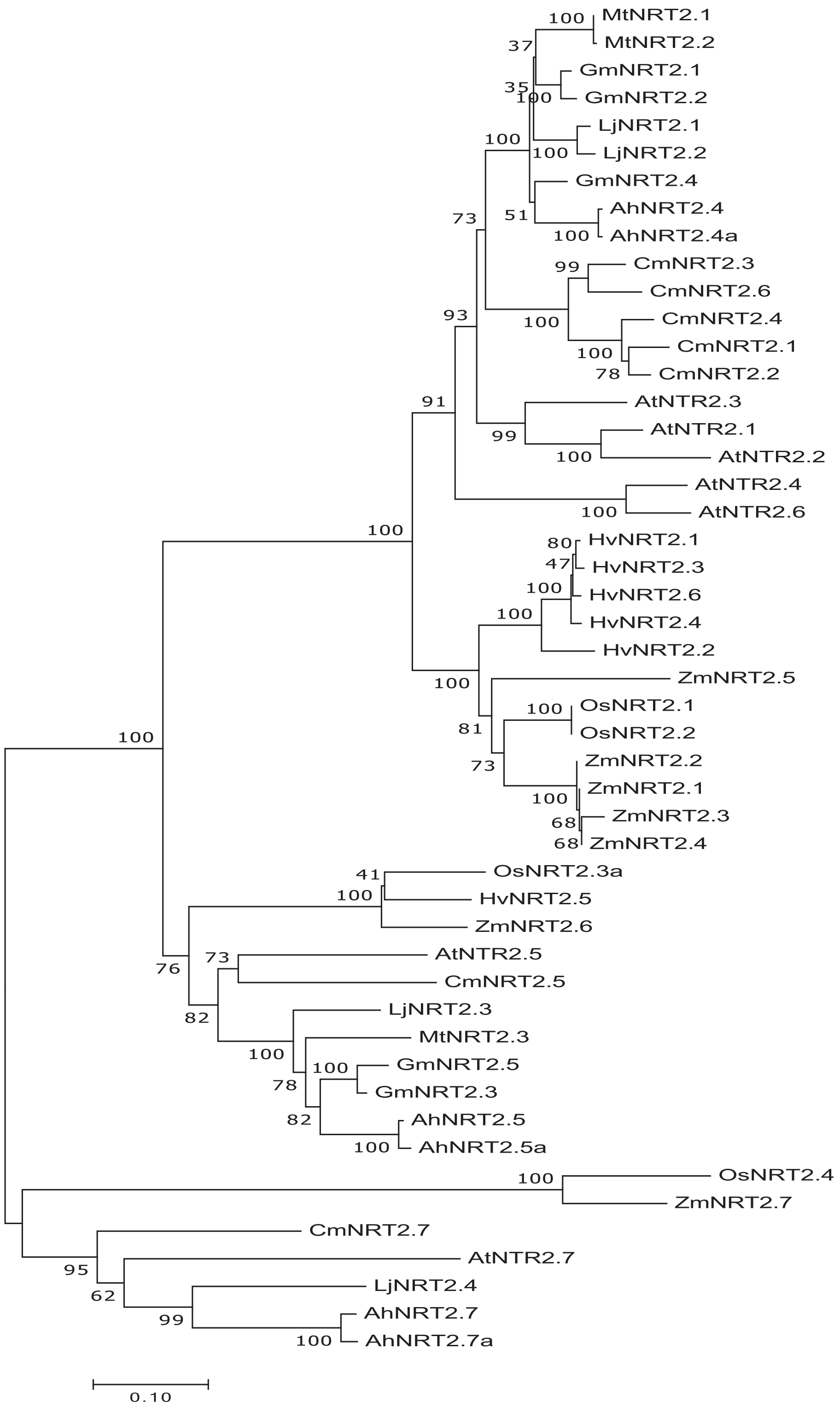

Fig. 1 Evolutionary relationships of plant Nitrate Transporter 2 (NRT2) families. Forty-nine full-length amino acid sequences were aligned with the ClustalW program. The evolutionary history was inferred using the Neighbor-Joining method (Saitou & Nei, 1987). The optimal tree with a sum of branch length = 4.97982140 is shown. The tree is drawn to scale, with branch lengths in the same units as those of the evolutionary distances used to infer the phylogenetic tree. Sequences are as follows: At, *Arabidopsis thaliana*; Ah, *Arachis hypogaea;* Cm, *Crysanthemum morifolium;* Gm, *Glycine max;* Hv, *Hordeum vulgare;* Lj, *Lotus japonicus;* Mt, *Medicago truncatula;* Os, *Oriza sativa;* Zm, *Zea mays*.

where a clear-cut induction of expression was described in young and mature nodular tissues. The *LjNRT2.4* transcript distribution in different organs of *L. japonicus* plants inoculated with *M. loti* confirmed the nodule-induced pattern (4.5-fold greater roots; Fig. 2). Furthermore, a striking peak of expression was found in mature dry seeds that is consistent with the analyses reported for the *AtNRT2.7* orthologue (Chopin *et al.*, 2007). However, the overall profile of expression observed in different organs (Fig. 2) is consistent with the results reported in the *L. japonicus* expression atlas (https://lotus.au.dk/expat/; Verdier *et al.*, 2013).

In order to gain further information about the profile of *LjNRT2.4* expression, a promoter-*gus*A translational fusion including 1038 bp upstream of the ATG and the first 10

© 2020 The Authors
New Phytologist © 2020 New Phytologist Trust

14698137, 2020, 2, Downloaded from https://nph.onlinelibrary.wiley.com/doi/10.1111/nph.16728 by CNR GROUP II Istituto di Scienza dell', Wiley Online Library on [23/05/2024]. See the Terms and Conditions (https://onlinelibrary.wiley.com/terms-and-conditions) on Wiley Online Library for rules of use; OA articles are governed by the applicable Creative Commons License

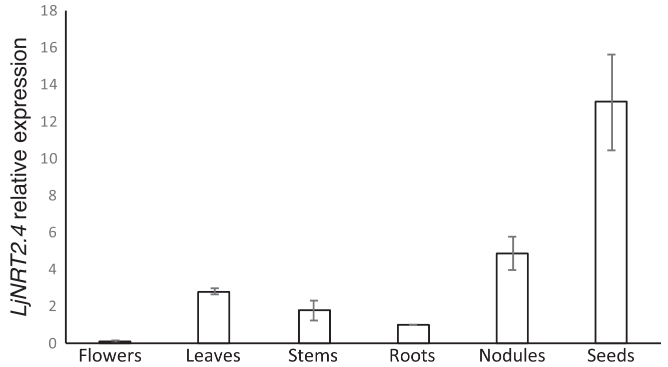

Fig. 2 *LjNRT2.4* transcriptional regulation in different *Lotus japonicus* organs (NRT, Nitrate Transporter). Mature flowers and seeds were obtained from lotus plants propagated in the growth chamber. Expression levels are normalized with respect to the internal control ubiquitin (*UBI*) gene and plotted as relative to the expression of roots. Data bars represent the mean ± SDs of data obtained with RNA extracted from three different sets of plants and three real-time PCR experiments.

LjNRT2.4 codons was exploited for obtaining nodulated hairy roots of *Lotus* composite plants upon transformation with *A. rhizogenes*. GUS activity was confined to vascular structures of roots and nodules with a higher intensity of the staining detected in the nodular tissue (Fig. 3a,b).

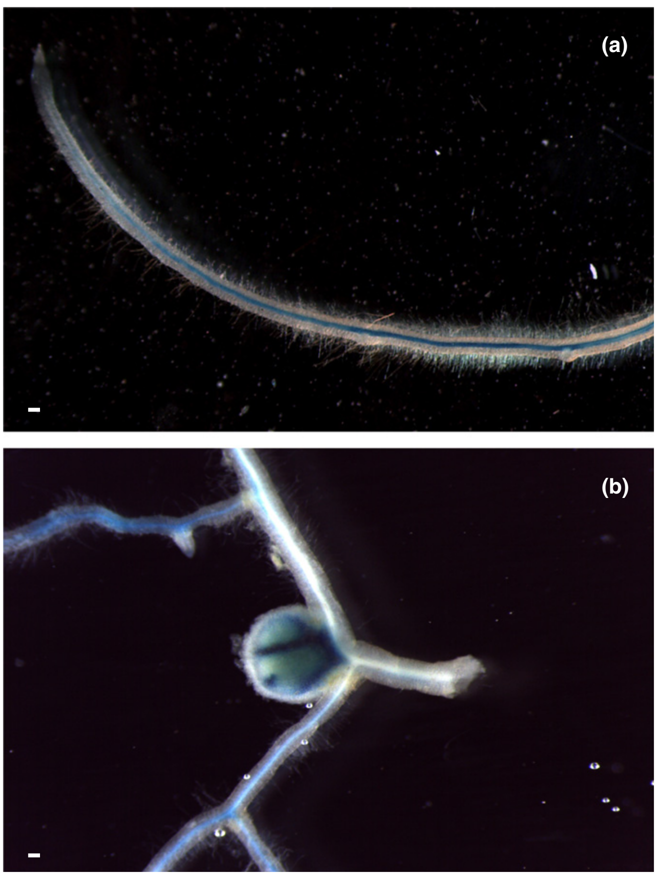

Fig. 3 Representative β-glucuronidase (GUS) activity of *Lotus japonicus* transgenic hairy roots transformed with the pr*LjNRT2.4-gus*A construct (NRT, Nitrate Transporter). (a) Staining in the root vascular bundle. (b) Staining in the nodule vascular bundles. Bars, 50 μm.

In order to determine the subcellular localization, we generated a fusion between the YFP and the N-terminus of LjNRT2.4 that was driven by the cauliflower mosaic virus 35S promoter. Confocal microscopy analysis in tobacco protoplasts indicated a localized fluorescence at the protoplast plasma membrane (Fig. 4).

Isolation of LORE1-insertion null mutants and phenotypic characterization

In order to determine the *in vivo* function of *LjNRT2.4*, two independent LORE1 insertion mutants were isolated from the released *L. japonicus* LORE1 lines collection (Fukai *et al.*, 2012; Urbanski *et al.*, 2012; Malolepszy *et al.*, 2016). Lines 30061917 and 30083188, bearing retrotransposon insertions in the first and second exon (Fig. 5a), were genotyped by PCR. Shoot cuts of homozygous plants for the insertion event into the *LjNRT2.4* gene were cultured in axenic conditions and then transferred to the growth chamber for seeds production. Endpoint RT-PCR analyses conducted with primers bracketing the insertion site of homozygous plants from lines 30061917 and 30083188 (hereafter called *Ljnrt2.4-1* and *Ljnrt2.4-2*, respectively) revealed no detectable *LjNRT2.4* full-size mRNA in nodules, and hence, these were considered null mutants (Fig. 5b). In order to analyze whether the induced pattern of expression in nodules reflected the involvement of LjNRT2.4 in the control of nodule efficiency we compared the phenotypes of wild-type (WT) and *Ljnrt2.4* mutants under symbiotic and nonsymbiotic conditions. The *Ljnrt2.4-1* and *Ljnrt2.4-2* mutants were grown in the presence of low KNO_3 concentration (100 μM) with/out *M. loti* inoculation and measurements of nodule number, shoot length and FWs of 4-wk-old plants were taken and compared to those of WT plants (Fig. 6). The mutant lines did not present significant differences when compared to WT plants, in terms of nodule number (Fig. 6a) as well as nodule size (data not shown). The invasion capacity of the *Ljnrt2.4* plants tested through inoculation with a *M. loti* strain carrying a constitutively expressed *hemA::lacZ* reporter gene revealed no differences with WT plants (Fig. S2). However, a slight significant difference was scored in the shoot biomass as both *Ljnrt2.4-1 and Ljnrt2.4-2* plants showed a significant 20% reduction in terms of shoot length and FW compared to WT plants (Fig. 6b,c). Consistently, this shoot biomass deficiency was coupled to a significant 20% reduction of nitrogenase activity detected in nodules detached at 4 wk post-inoculation (Fig. 6d). Furthermore, a very clear stressful phenotype displayed by the mutants and detected only in symbiotic conditions comprised a clear-cut accumulation of anthocyanin, conferring deep purple colour in the stems. The correlation between anthocyanin accumulation and the nodulation process in the mutant plants was demonstrated strikingly by the experiment shown in Fig. 7. Plants were first grown for 10 d in the presence of 2.5 mM KNO_3 as sole N source showing no evident phenotypes. Both WT and *Ljnrt2.4* plants grown in the same Petri dishes displayed similar shoot height and no stress symptoms (Fig. 7a). Subsequently, plants were transferred to media with no N sources or 100 μM KNO_3 and inoculated with *M. loti*. Twelve days post-inoculation, red nodules were clearly visible at the same density

© 2020 The Authors
New Phytologist © 2020 New Phytologist Trust

14698137, 2020, 2, Downloaded from https://nph.onlinelibrary.wiley.com/doi/10.1111/nph.16728 by CNR GROUP II Istituto di Scienza dell', Wiley Online Library on [23/05/2024]. See the Terms and Conditions (https://onlinelibrary.wiley.com/terms-and-conditions) on Wiley Online Library for rules of use; OA articles are governed by the applicable Creative Commons License

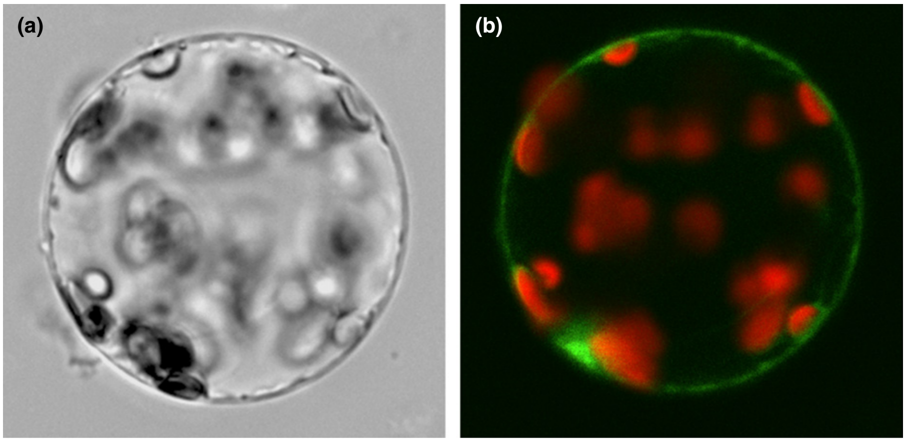

Fig. 4 *Lotus japonicus* NRT2.4 localization at the plasma membrane. The YFP-LjNRT2.4 translational fusion was transiently expressed in protoplast of tobacco mesophyll cells under the control of the 35S promoter. (a) Bright field image of tobacco protoplast. (b) Merged image of yellow fluorescent protein (YFP) and chlorophyll autofluorescence in transformed protoplasts.

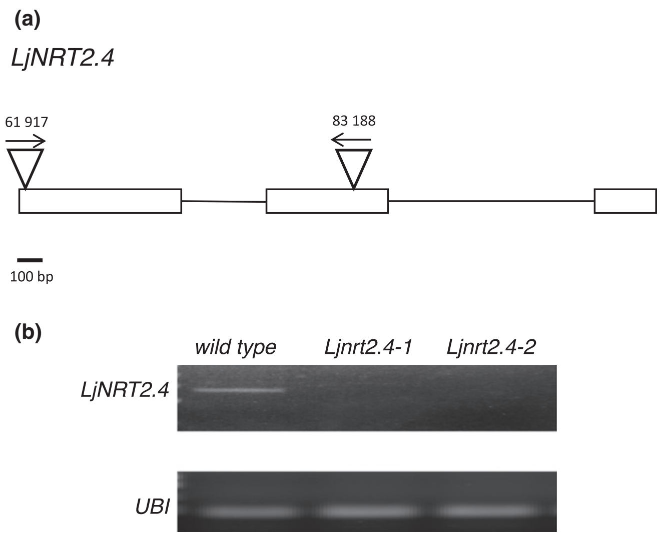

Fig. 5 Structure of the *Lotus japonicus* NRT2.4 gene and analysis of the expression in the LORE1 segregants (NRT, Nitrate Transporter). (a) Exon/intron organization of the *LjNRT2.4* gene. Insertion sites and relative orientations of the LORE1 retrotransposon element in the 30 061 917 and 30 083 188 lines are indicated. (b) Expression of the LjNRT2.4 gene in the *Ljnrt2.4-1* and *Ljnrt2.4-2* plants. Total RNAs isolated from nodules has been used for real-time PCR analysis.

on the younger part of the root system of both WT and *Ljnrt2.4* plants and the two mutants showed an extensive anthocyanin accumulation in the stem tissues compared to WT plants (Fig. 7b). The quantitative analysis performed through anthocyanin extraction from stem tissues confirmed a content 2.5–3-fold higher in stems of the mutants compared to WT plants, whereas no significant differences were scored in noninoculated plants (Fig. 7c). In the phenotypic characterizations described above, two individual homozygous mutant plants from both *Ljnrt2.4-1* and *Ljnrt2.4-2* lines were analyzed and because their growth phenotypes did not significantly differ, the data obtained with the selected individual mutants have been pooled in this study. The identical phenotypes displayed by the *Ljnrt2.4-1* and *Ljnrt2.4-2* mutants confirm that the LORE1 insertions in the *LjNRT2.4* gene are the causal mutations of the deficient phenotype scored in symbiotic conditions. In addition, heterozygous plants for the LORE1 insertion in the *LjNRT2.4* gene isolated in the two lines, did not display the high concentration of anthocyanin in the stem (data not shown).

The deficient symbiotic phenotypes of the *Ljnrt2.4* mutants become much more severe in plants grown under hydroponic conditions

A significant reduction of the nodule nitrogenase activity was reported in nodules of soybean plants subjected to flooding conditions (Sanchez *et al.*, 2010). Flooding imposes stress on plants by severely hampering gas exchange and reducing oxygen internal pressure (hypoxia). Likewise, nitrate was demonstrated to play a very stringent role in the maintenance of the nodule energy in hypoxic conditions (Horchani *et al.*, 2011; Hicri *et al.*, 2015). Therefore, in order to test whether the deficient symbiotic phenotype displayed by the *Ljnrt2.4* plants was more severe in hypoxic conditions we compared the phenotypes of nodulated WT and mutant plants under hydroponic conditions. Wild-type and *Ljntr2.4* seeds were germinated on solid medium, and at 4 d post-inoculation seedlings were transferred into hydroponic cultures, in the presence of 100 µM KNO_3 as sole N source. At 5 wk post-inoculation, both *Ljnrt2.4-1* and *Ljnrt2.4-2* plants displayed a striking stunted shoot phenotype with clear-cut N starvation chlorosis symptoms (Fig. 8a). By comparison, parallel inoculated *Ljnrt2.4* plants grown on clay granules (normoxic conditions) did not show a similar shoot biomass defect when compared to WT plants although the slight reduction of FW reported in axenic conditions was confirmed (Fig. S3).

Ljnrt2.4 nodules are impaired in N_2-fixation activity, nitrate content and nitrate-dependent NO biosynthetic pathway

The direct analyses of N_2-fixation activities of nodules from plants grown in hydroponic conditions indicated a stronger reduction of N_2-fixation capacity in both *Ljnrt2.4* vs wild-type plants (Fig. 8b) compared to the differences scored in axenic conditions (Fig. 6d). In particular, a 50% reduction of ARA activity was measured in the mutant nodules that could be responsible for the severe N-starvation phenotype detected in hydroponic

© 2020 The Authors
New Phytologist © 2020 New Phytologist Trust

14698137, 2020, 2, Downloaded from https://nph.onlinelibrary.wiley.com/doi/10.1111/nph.16728 by CNR GROUP II Istituto di Scienza dell', Wiley Online Library on [23/05/2024]. See the Terms and Conditions (https://onlinelibrary.wiley.com/terms-and-conditions) on Wiley Online Library for rules of use; OA articles are governed by the applicable Creative Commons License

14698137, 2020, 2, Downloaded from https://nph.onlinelibrary.wiley.com/doi/10.1111/nph.16728 by CNR GROUP II Istituto di Scienza dell', Wiley Online Library on [23/05/2024]. See the Terms and Conditions (https://onlinelibrary.wiley.com/terms-and-conditions) on Wiley Online Library for rules of use; OA articles are governed by the applicable Creative Commons License

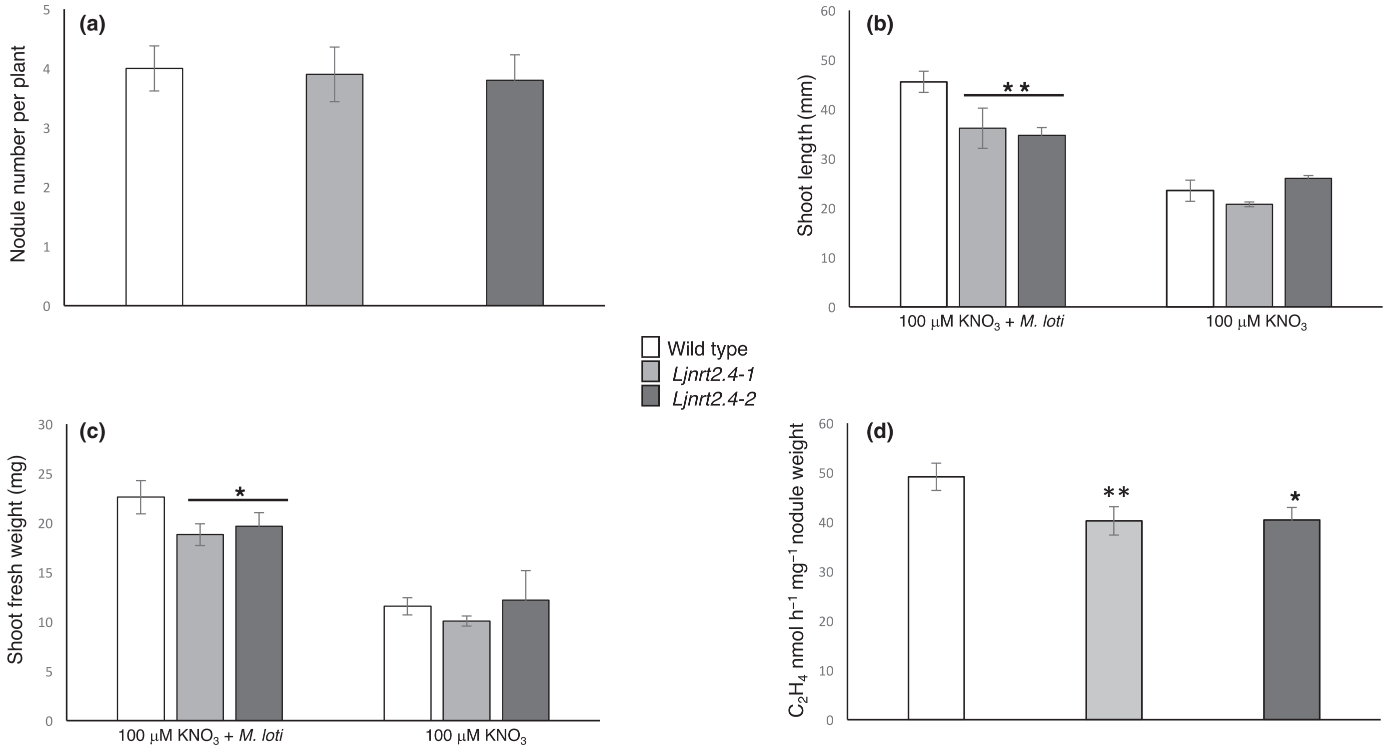

Fig. 6 Phenotypic characterization of *Lotus japonicus Ljnrt2.4-1* and *Ljnrt2.4-2* mutants (NRT, Nitrate Transporter). Wild-type (WT) and *Ljnrt2.4* plants, were grown in the presence of 100 μM KNO_3, in symbiotic and nonsymbiotic conditions. (a) Nodule numbers per plant. Nodules were scored at 4 wk post-inoculation (wpi). (b) Shoot length per plant. (c) Fresh shoot weight per plant. (d) Acetylene Reduction Activity (ARA) per nodule weight. Bars represent means ± SE of measures from three experiments (12 plants per experiment per condition). Asterisks indicate significant differences with WT levels: *, $P < 0.05$; **, $P < 0.03$.

cultures. This result confirmed a positive role of LjNRT2.4 on nodule functioning that became more stringent in hypoxic conditions. In order to develop a mechanistic model for explaining the observed phenotype in hydroponic conditions, nodules detached from roots of plants grown in hydroponic conditions in the presence of low nitrate concentrations (100 μM KNO_3) were analyzed for nitrate content. The values obtained for the nitrate content in *Ljnrt2.4-1* and *-2* nodules were significantly reduced compared to the WT by 38% and 75%, respectively (Fig. 9a). Interestingly a similar, significant reduction of the nitrate content was detected in the mutant nodules in plants grown on a clay granules (normoxic condition) (Fig. 9a). These results suggest a role of the LjNRT2.4 protein in the allocation of nitrate to the nodules, indicating a more stringent role of a correct nitrate content for nodule efficiency under hypoxic than normoxic conditions. The role of LjNRT2.4 in the nitrate content of the nodules prompted us to investigate whether it could be involved in the nitrate inhibitory pathway affecting N_2-fixation activity. Nodulated plants grown for 3 wk in the presence of 100 μM KNO_3 were shifted for 48 h in 10 mM KNO_3 and N_2-fixation activity was evaluated through ARA assay. As expected, the nitrogenase activity was inhibited of almost 50% after the shift in WT nodules, and a similar reduction was scored in the *Ljnrt2.4* nodules (data not shown).

In order to test whether the reduced nitrate content detected in the mutant nodules was correlated to a lower capacity of NO production, we decided to make quantitative measures on the whole nodules to avoid artefact owing to NO production as result of mechanical stress (Horchani *et al*., 2011). The NO produced and released from entire nodules still attached to a small piece of root (extending *c*. 0.2 cm at both sides of the nodules) was scored through incubation in a medium containing the DAF probe. The production of NO was measured by incubating the samples under normal (21% O_2, normoxic) and low oxygen pressure (1% O_2, hypoxic). As expected the NO production in the WT nodules was significantly increased under low oxygen pressure (Horchani *et al*., 2011) and the values increased in a linear way at least ≤ 4 h (Fig. 9b). Interestingly, when we compared the NO production in WT and mutant nodules, the latter show significantly reduced values (*c*. 30%). It must be taken into consideration that the different absolute values of NO production recorded in Fig. 9(c) probably result from a little intrinsic experimental variability with a delayed scoring of NO production in the experiment shown in Fig. 9(b). Furthermore, the differences in NO production were strongly confirmed by the comparison of the NO content in nodules of WT and *Ljnrt2.4* plants grown in hydroponic conditions, showing a significantly reduced proportion of NO (*c*. 45%) in nodules of the *Ljnrt2.4* plants (Fig. 9d).

Discussion

To date, the role of nitrate as regulator of symbiotic N_2 fixation (SNF) has been investigated only to understand the inhibitory role exerted by high external concentrations of this nutrient on

© 2020 The Authors
New Phytologist © 2020 New Phytologist Trust

14698137, 2020, 2, Downloaded from https://nph.onlinelibrary.wiley.com/doi/10.1111/nph.16728 by CNR GROUP II Istituto di Scienza dell', Wiley Online Library on [23/05/2024]. See the Terms and Conditions (https://onlinelibrary.wiley.com/terms-and-conditions) on Wiley Online Library for rules of use; OA articles are governed by the applicable Creative Commons License

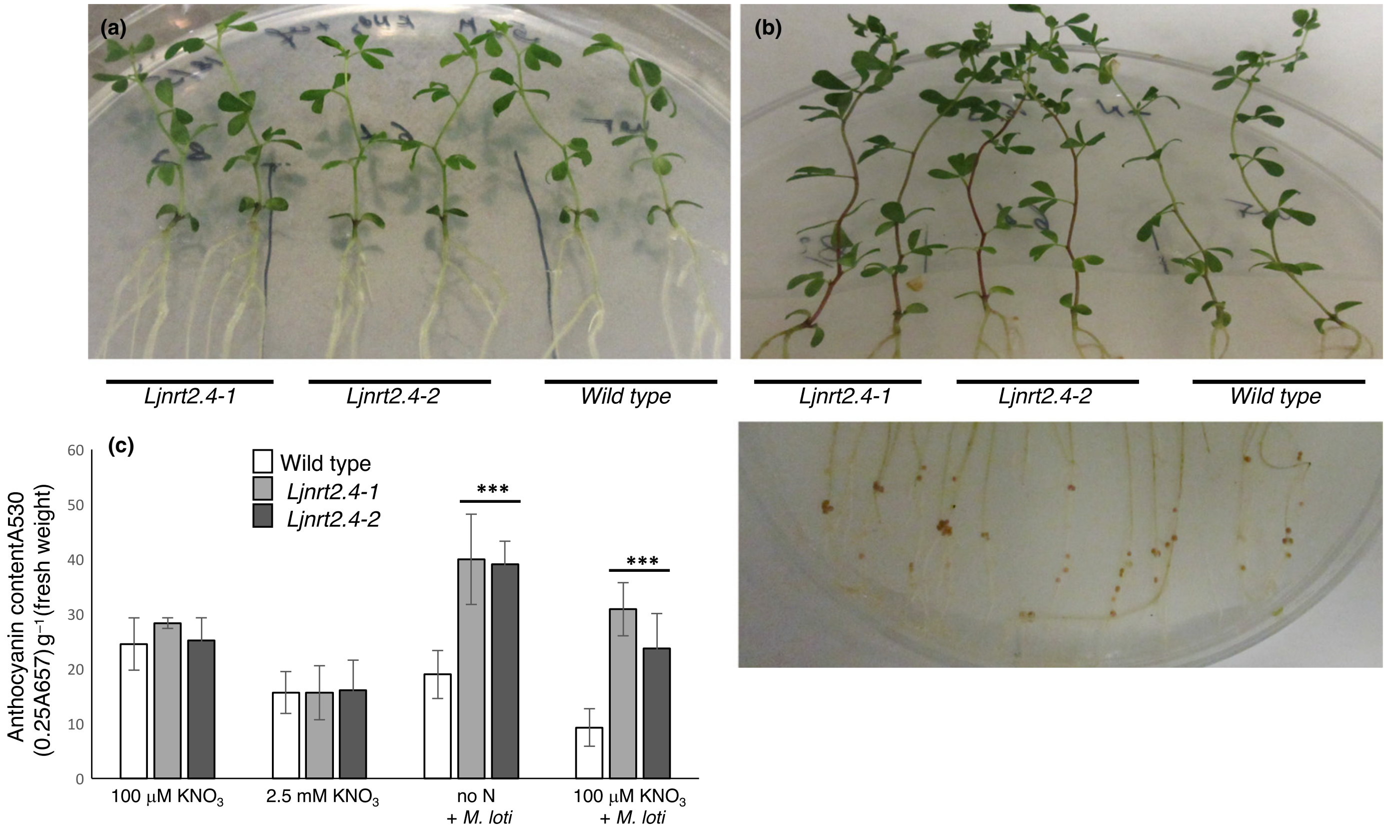

Fig. 7 Anthocyanin accumulation in *Lotus japonicus* under symbiotic conditions. (a) Representative wild-type (WT), *Ljnrt2.4-1* and *Ljnrt2.4-2* plants grown on 2.5 mM KNO_3 for 10 d (NRT, Nitrate Transporter). (b) Shoots (up) and roots (bottom) of the plants shown in (a), post-inoculation with *Mesorhizobium loti* and incubation for additional 12 d on no N conditions. (c) Anthocyanin content. The different KNO_3 concentrations and when performed, *M. loti* inoculation, are indicated. Bars represent means ± SE of measures from three experiments (12 plants per experiment per condition). Asterisks indicate significant differences ($P < 0.001$) with Wt levels.

all of the different steps of nodule formation, development and functioning (Carroll & Gresshoff, 1983; Fujikake *et al*., 2003; Barbulova *et al*., 2007; Omrane & Chiurazzi, 2009; Jeudy *et al*., 2010; Cabeza *et al*., 2014). However, only little attention has been paid to the potential positive role of low, permissive external concentrations of nitrate, and how this can act to modulate nodulation capacity and functioning. A positive role of low nitrate external concentrations on nodule formation capacity has been reported in *Lotus japonicus* and other legumes (Hussain *et al*., 1999; Barbulova *et al*., 2007). In the same way, a nitrate-dependent respiratory chain aimed to maintain the energy status required for efficient N_2-fixation has been reported (Horchani *et al*., 2011; Hicri *et al*., 2015). We report here the functional characterization of the *LjNRT2.4* gene that revealed its positive role in a nitrate-mediated nodule functioning pathway.

The phylogenetic tree shown in Fig. 1 confirmed the divergence of the AtNRT2.7-like genes in the frame of the plant NRT2 members. The absence of AtNRT2.7 orthologue already has been reported for grass genomes, poplar and *Medicago truncatula* (Plett *et al*., 2010; Pellizzaro *et al*., 2015). This scattered distribution of the NRT2.7-like gene among the plant NRT2 families, even among strictly related legume species such as *L. japonicus, M. truncatula* and *Glycine max,* clearly indicated an independent evolution for this gene. The functional characterization of the NRT2.7-like genes has been carried out in *Arabidopsis thaliana* and *Oryza sativa*, confirming very specialized roles. *AtNRT2.7* is peculiar among the *Arabidopsis NRT2* genes as it is expressed mainly in the seeds where it is involved in the control of nitrate accumulation and seed germination. AtNRT2.7 displays a unique vacuolar subcellular localization (Chopin *et al*., 2007), compared to all of the other *Arabidopsis* members showing a plasma membrane (PM) localization and expressed mainly in root tissues. *OsNRT2.4* is not expressed in the embryo but it is the only rice *NRT2* member expressed mainly in the shoot. A PM localization has been reported for OsNRT2.4, consistent with the other rice NRT2 proteins. However, both AtNRT2.7 and OsNRT2.4 have the unique capacity to not require the NAR2 accessory protein for nitrate transport (Kotur *et al*., 2012). Furthermore, both are involved in the nitrate mobilization from source to sink tissues, the seeds in the case of AtNRT2.7 (Chopin *et al*., 2007), and young leaves and roots for OsNRT2.4 (Wei *et al*., 2018). The strong induction of expression of *LjNRT2.4* in nodular tissue compared to root reported in Figs 2 and 3 also is peculiar among the *Lotus NRT2* genes (Criscuolo *et al*., 2012). It will be interesting to investigate whether, when present, NRT2-like genes in other legume species display the same nodule-induced pattern. In the case of the *AhNRT2.7* identified in the legume *A. hypogaea* we could not

© 2020 The Authors
New Phytologist © 2020 New Phytologist Trust

14698137, 2020, 2, Downloaded from https://nph.onlinelibrary.wiley.com/doi/10.1111/nph.16728 by CNR GROUP II Istituto di Scienza dell', Wiley Online Library on [23/05/2024]. See the Terms and Conditions (https://onlinelibrary.wiley.com/terms-and-conditions) on Wiley Online Library for rules of use; OA articles are governed by the applicable Creative Commons License

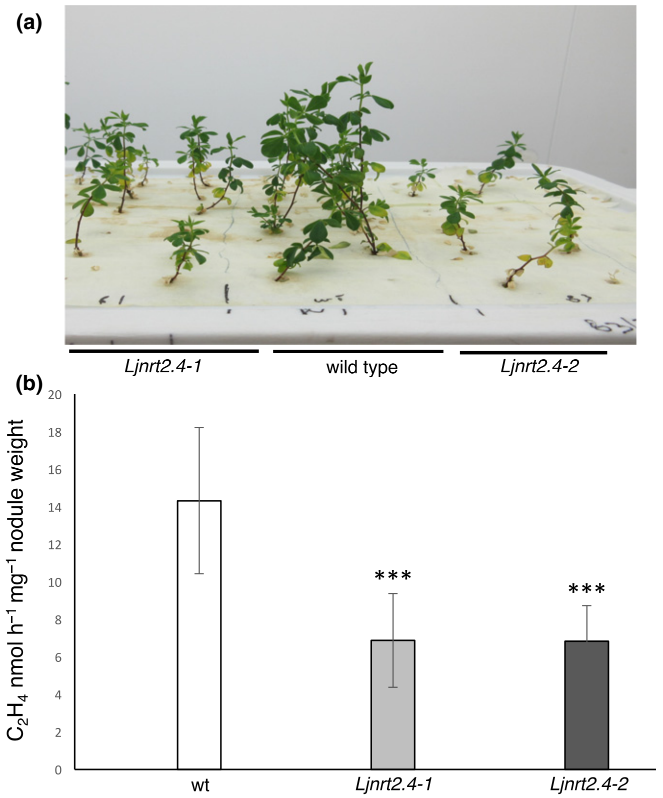

Fig. 8 *Lotus japonicus* phenotypic characterization in hydroponic conditions. (a) Representative images of wild-type, *Ljnrt2.4-1* and *Ljnrt2.4-2* plants maintained under 100 μM KNO_3 conditions at 5 wk after inoculation with *Mesorhizobium loti* (NRT, Nitrate Transporter). (b) Acetylene Reduction Activity (ARA) per nodule weight. Data bars indicate the mean ± SE of three independent experiments ($n = 8$ plants per experiment). Asterisks indicate significant differences ($P < 0.001$).

retrieve reliable gene atlas data to confirm an induction in the nodules. Interestingly, nodules also are optional sink organs as these need to assimilate energy sources to provide energy for the N_2-fixation activity performed by the microsymbiont as well as assimilation of the produced ammonium and starch biosynthesis (Vance, 2008).

The phenotypes of the two independent knock-out mutants shown in Figs 6–8 clearly highlighted the action played by LjNRT2-4 for a correct functioning of N_2-fixing nodules. The lack of altered phenotypes shown by *Ljnrt2.4-1* and *-2* during the growth in nonsymbiotic conditions (Fig. 6), as well as their normal capacity of nodule formation and development (Figs 6a, S3), indicated a specialized role of LjNRT2.4 that takes place during nodule functioning, consistent with its temporal and spatial profile of expression (Figs 2, 3). In particular, the striking anthocyanin accumulation detected in the stems of the *Ljnrt2.4* plants that is not observed in the uninoculated plants confirmed the involvement of LjNRT2.4 in the nodule-functioning process. The stem pigmentation represents a clear-cut N-limitation stress symptom associated to an impaired N_2-fixation activity (Krussell *et al.*, 2005; Ott *et al.*, 2005; Bourcy *et al.*, 2013). The small reduction of shoot height and weight scored in the mutants (Fig. 6b,c) might be explained by the partial impairment of nitrogenase activity reported in Fig. 6(d). These phenotypes resemble the ones of the Fix^+/Fix^- mutants showing a less efficient N_2-fixation activity, which display N-deficiency phenotypes not as severe as those of *fix*$^-$ mutants (Pislariu *et al.*, 2012). However, the mild phenotype exhibited by the *Ljnrt2.4* plants turned to a much more severe one under hydroponic conditions, where a clear-cut N-starvation shoot phenotype was scored, associated with a stronger reduction of the nitrogenase activity when compared to wild-type (WT) plants (Fig. 8). The absolute level of nodule nitrogenase activity was reduced about three times in hydroponic vs axenic conditions (Figs 6d, 8b). A similar reduction of nitrogenase activity was reported in soybean nodules of plants subjected to flooding conditions (Sanchez *et al.*, 2010). Our phenotypic characterization also indicated an increase of nitric oxide (NO) production when nodules were analyzed under hypoxic vs normoxic conditions (Fig. 9b). Interestingly, a significant reduction of NO production was detected in mutant nodules analyzed under hypoxic conditions when compared to WT nodules (Fig. 9c). Finally, the decreased capacity of NO production in the *Ljnrt2.4* mutants was directly confirmed by scoring the NO content of detached nodules obtained from hydroponic cultures (Fig. 9d). Nitric oxide accumulation under flooding conditions has been reported in WT *M. truncatula* and soybean mature nodules as well as isolated bacteroids, together with nitrite (NO_2^-) accumulation (Meakin *et al.*, 2007; Sanchez *et al.*, 2010). A free radical, gaseous molecule, NO is involved in a wide spectrum of regulatory functions in plant growth and development, and response to stress conditions. The NO production during different steps of the legume–*rhizobium* symbiotic interaction has been demonstrated in different reports (Meakin *et al.*, 2007; Nagata *et al.*, 2008; Sanchez *et al.*, 2010; del Giudice *et al.*, 2011) and NO accumulation was confined to the region of bacteroid-containing cells in mature nodules (Baudouin *et al.*, 2006; Shimoda *et al.*, 2009; Meilhoc *et al.*, 2010). Both partners in the plant cell cytosol and bacteroid compartments of N_2-fixing invaded cells can produce NO. In the bacteroid compartment the main route for NO production is considered the denitrification pathway, whereas in the plant cell cytosol, genetic evidences indicate the nitrate reductase-mediated pathway as the main source of NO (Horchani *et al.*, 2011). The use of different inhibitors of the mitochondrial and bacteroid electron transfer chain (ETCs) indicated that both are involved in NO production (Horchani *et al.*, 2011). The role of NO in the N_2-fixing nodules is still a matter of debate. During N_2-fixation, as in other developmental and stress response processes, a finely tuned control of NO homeostasis is a crucial step to determine local NO concentration and effects. The NO-dependent inhibition of nitrogenase activity that is likely occurring through a S-nitrosylation post-translational modification has been reported in soybean, *L. japonicus* and *M. truncatula* nodules (Trinchant & Rigaud, 1982; Puppo *et al.*, 2005; Shimoda *et al.*, 2009; Kato *et al.*, 2010; Cam *et al.*, 2012). However, the reported effects of NO donors and scavengers on Acetylene Reduction Activity (ARA) activity of *Lotus* nodules indicated that a low but significant NO content is necessary for nitrogenase activity (Kato *et al.*, 2010). Furthermore, in *M. truncatula* a positive role of a nitrate-NO respiration process has been reported, where NO_2^- might act as an electron acceptor

© 2020 The Authors
New Phytologist © 2020 New Phytologist Trust

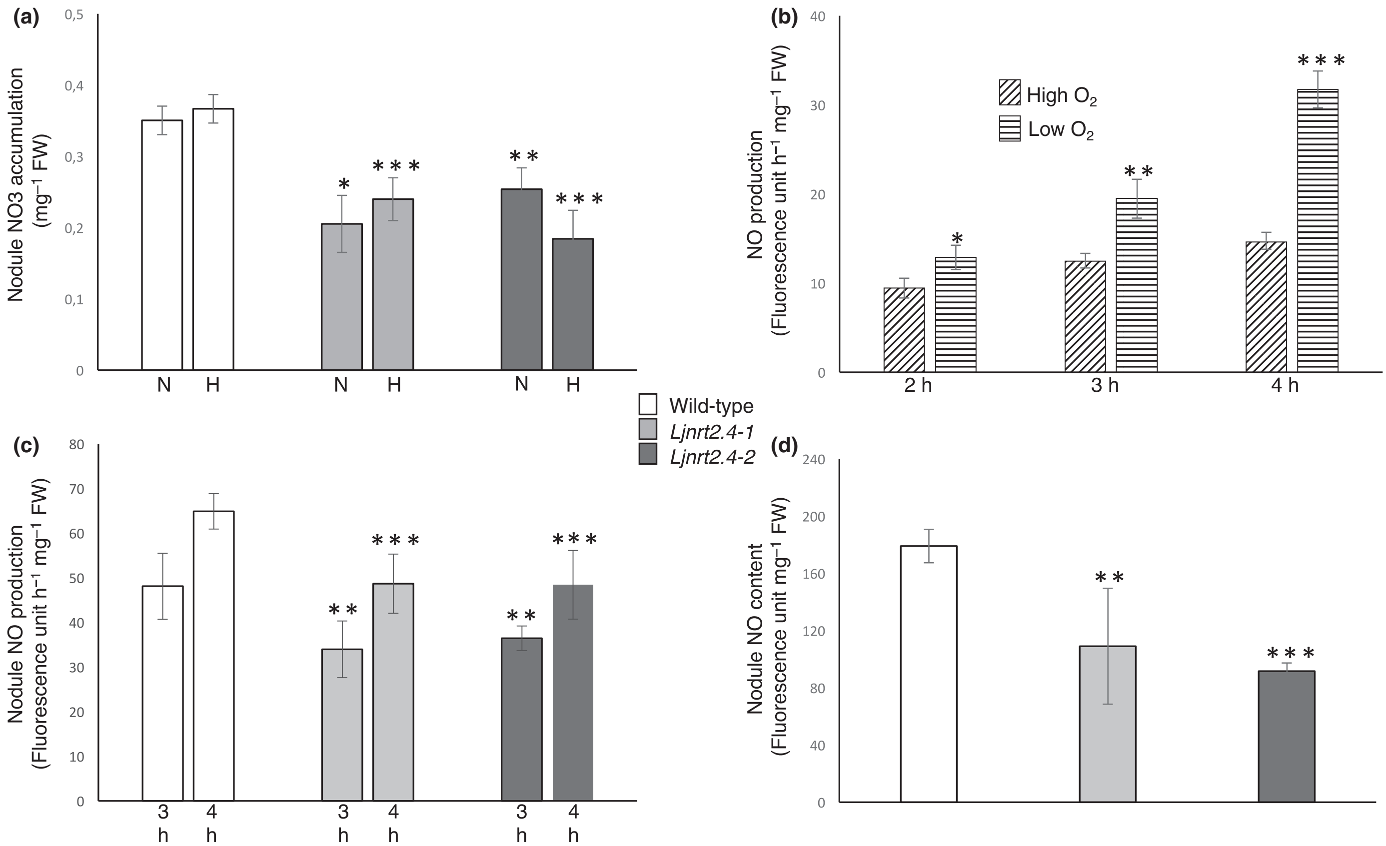

Fig. 9 *Lotus japonicus* nitrate and nitric oxide (NO) scoring in nodules. (a) Nodule nitrate content of wild-type (WT) and *Ljnrt2.4* nodules (NRT, Nitrate Transporter). Plants were grown either in pots with clay granules (N = normoxic conditions) and hydroponic conditions (H) in the presence of 100 μM KNO_3. (b) NO time course production in detached WT nodules assayed under 21% (high) and 1% (low) oxygen. The times (h) of the NO scoring are indicated. (c) NO nodule production assay under low oxygen conditions. The WT and *Ljnrt2.4* plants were grown in the presence of 100 μM KNO_3. The times (h) of the NO scoring are indicated. (d) NO content in nodules of WT and *Ljnrt2.4* plants grown under hydroponic conditions in the presence of 100 μM KNO_3. Data bars represent means ± SE from three independent experiments (seven plants per experiment with two nodule samples/experiment scored for NO production). Asterisks in (a), (c) and (d) indicate significant differences with WT levels. Asterisks in (b) indicate significant differences between low and high oxygen. *, $P < 0.05$; **, $P < 0.03$; ***, $P < 0.01$.

instead of oxygen, playing a role in the maintenance of the energy status required for N_2-fixation (Horchani *et al.*, 2011). The nitrate-NO respiration cycle in the nodule-invaded cells is characterized by four steps: NO_3 reduction by NR; NO_2^- translocation to the mitochondrial and peryplasmic ETCs; NO_2^- reduction to NO for ATP regeneration; and passive diffusion of NO that is oxidized again by Leghemoglobin and flavohemoglobin (Fig. 10; Hicri *et al.*, 2015). This nitrate-dependent route for NO production is essential in hydroponic, hypoxic conditions, when the oxygen concentration can become limiting for supporting the full nitrogenase activity required to satisfy N demands in the presence of low concentrations of nitrate. It is reasonable to postulate that this NO-producing route in the nodule might need or be supported by allocation of nitrate to the nodules. The phenotypes observed with the *Ljnrt2.4* plants are certainly consistent with such a function. Although we did not perform a biochemical characterization to directly demonstrate the role of LjNRT2.4 as nitrate transporter, its involvement in the nitrate loading of nodules is suggested by the significantly reduced nitrate content scored in the nodules of the mutant genotypes (Fig. 9a). The tissue localization in the nodule vascular bundles (Fig. 3b) as well as its plasma membrane subcellular localization (Fig. 4) also are consistent with such a role. It is also important to take in consideration that, when investigated either in heterologous or *in planta* experimental systems, a direct correlation always has been found, without any exception, between nitrate uptake activity and plant NRT2 proteins. The nitrate transport capacity has been reported for the whole family of *A. thaliana* and *O. sativa* NRT2 proteins (Wei *et al.*, 2018; Wang *et al.*, 2018), as well as for the characterized NRT2 members of *Brassica napus, Lycopersicon esculentum, Chrysanthemum morifolium, Cucumis sativa, Cassava* and *Brachypodium distachyon* (Leblanc *et al.*, 2013; Fu *et al.*, 2015; Gu *et al.*, 2016; Li *et al.*, 2018; Wang *et al.*, 2019; L. Zou *et al.*, 2019). Furthermore, specific links between altered *NRT2* gene expression obtained in mutant or overexpressing genetic backgrounds and nitrate-related plant phenotypes havebeen reported in many plants, including *Triticum aestivum* and *Zea mays* (Fu *et al.*, 2015; He *et al.*, 2015; Taulemesse *et al.*, 2015; Gu *et al.*, 2016; Ibrahim *et al.*, 2017; Wei *et al.*, 2018; Li *et al.*, 2018; Wang *et al.*, 2018; Naz *et al.*, 2019; L. Zou *et al.*, 2019; Luo *et al.*, 2020). The reduced NO production and content detected in the *Ljnrt2.4* nodules are

© 2020 The Authors
New Phytologist © 2020 New Phytologist Trust

14698137, 2020, 2, Downloaded from https://nph.onlinelibrary.wiley.com/doi/10.1111/nph.16728 by CNR GROUP II Istituto di Scienza dell', Wiley Online Library on [23/05/2024]. See the Terms and Conditions (https://onlinelibrary.wiley.com/terms-and-conditions) on Wiley Online Library for rules of use; OA articles are governed by the applicable Creative Commons License

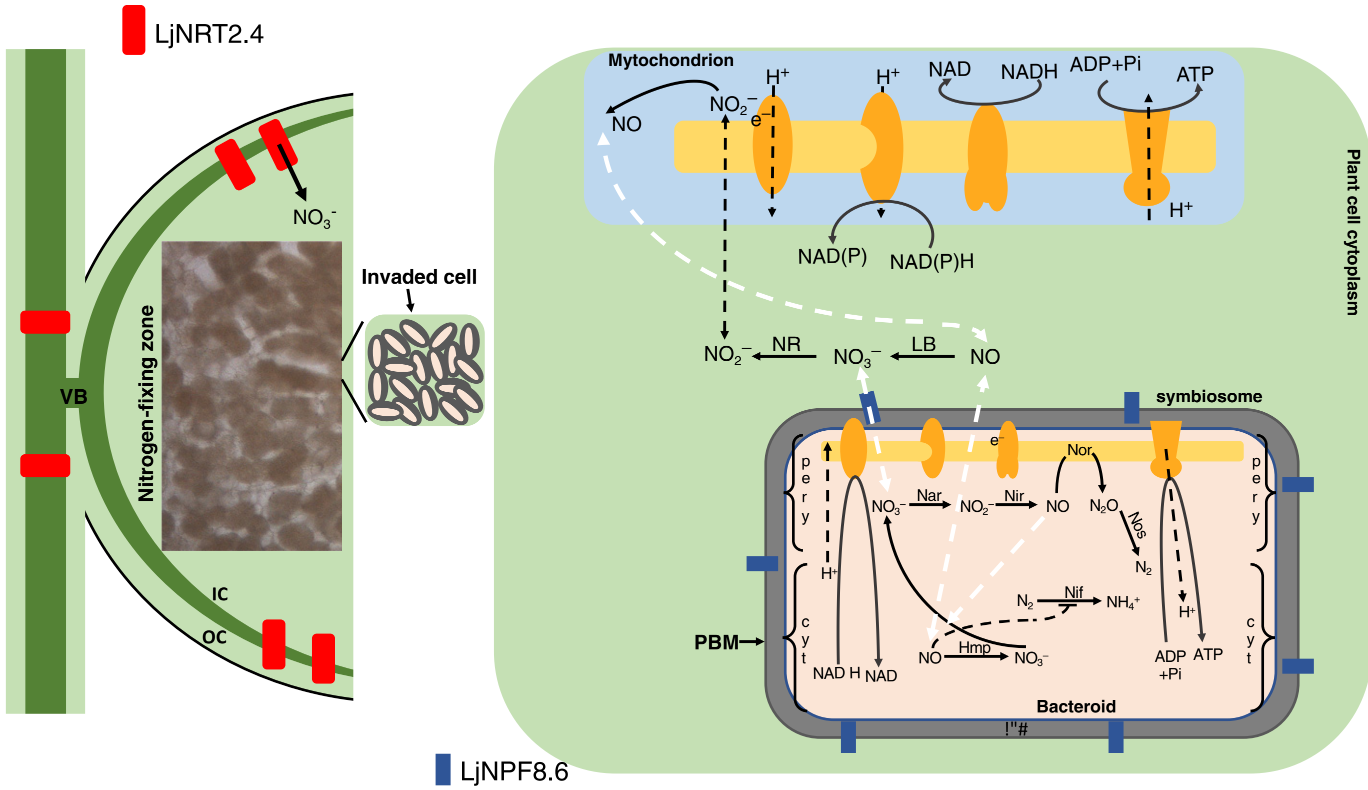

Fig. 10 Scheme of the model of nitrate allocation to the N_2-fixing zone of the *Lotus japonicus* nodules and its utilization for the nitrate-nitric oxide (NO) respiration cycle occurring in the invaded cells. On the left is highlighted the putative role of LjNRT2.4 (in red) for allocation of nitrate to the N_2-fixing cells (NRT, Nitrate Transporter). On the right, a single invaded cell is schematized where NO_3^- reduction to NO_2^- takes place in both the compartments via nitrate reductase activity. In the plant cytosol, NO_2^- is transferred to the mythocondria where it functions as an alternative electron acceptor in the electron transport chain (ETC), being further reduced to NO and allowing ATP regeneration. In the bacteroid compartment, NO is produced through the denitrification pathway and ATP is synthetized at the periplasmic ETC. The cycle is completed by NO oxidation to NO_3^- that takes place by means of leghemogobin and flavohemoglobin in the plant cytosol and bacteroid compartments, respectively. Dotted white lines indicate putative movements of molecules. The putative role of the low-affinity nitrate transporter LjNPF8.6 (in blue) to regulate the nitrate flux between plant cell cytosol and bacteroid compartments is indicated (Valkov *et al*., 2017). VB, vascular bundle; IC, internal cortex; OC, outer cortex; PBM, peri-bacteroide membrane; PBS, peri-bacteroide space; NR, nitrate reductase; LB, leghemoglobin; Nar, nitrate reductase; Nir, nitrite reductase; Nor, NO reductase; Hmp, flavohemoglobin; Nif, nitrogenase. Adapted from Horchani *et al*. (2011).

consistent with a deficient support of the nitrate substrate (Fig. 9b–d). The two knock-out mutants showed a N-starvation phenotype, associated with an impaired N_2-fixation activity that is severely increased under hydroponic conditions, when the nitrate-NO respiratory cycle is enhanced. Interestingly, the AtNRT2.7 nitrate transporter also has a postulated role in the NO production pathway taking place in the seeds under anaerobic or dark conditions that could link the nitrate content controlled by AtNRT2.7 and seed dormancy (Bethke *et al.*, 2006; Chopin *et al.*, 2007).

Nitrate Transporter Peptide (NPF) and NRT2 proteins are largely represented among the categories of transporters induced in the mature nodules (Valkov & Chiurazzi, 2014; Clarke *et al.*, 2015). In particular, a large number of NPF proteins are represented in the protein fraction associated with the peri-bacteroidal membrane in soybean nodules (Clarke *et al.*, 2015). We have already proposed the involvement of the LjNPF8.6 in the functioning of the NO-based respiratory cycle schematized in Fig. 10, where this member could play a role in the control of the nitrate flux between cytosolic and bacteroids compartments of N_2-fixing cells (Valkov *et al.*, 2017). Therefore, we hypothesize that *NPF* and *NRT2* genes have complementary functions for ensuring the functioning of a nitrate-dependent pathway that becomes limiting under hypoxic conditions.

Acknowledgements

We thank Danilo Maiello, Marco Petruzziello and Giuseppina Zampi for technical assistance. This work was supported by grant from the Italian Ministery of the Economic Development (MISE), Sviluppo di nuove piattaforme molecolari/cellulari per l'identificazione e lo sviluppo di principi attivi innovative, sostenibili e di origine naturale per l'applicazione cosmetica-F/050005/00/X32 and by CNR project FOE-2019 DBA.AD003.139.

Author contributions

VTV designed, performed and analyzed the experiments; SS designed and performed the experiments; AR designed and

© 2020 The Authors
New Phytologist © 2020 New Phytologist Trust

14698137, 2020, 2, Downloaded from https://nph.onlinelibrary.wiley.com/doi/10.1111/nph.16728 by CNR GROUP II Istituto di Scienza dell', Wiley Online Library on [23/05/2024]. See the Terms and Conditions (https://onlinelibrary.wiley.com/terms-and-conditions) on Wiley Online Library for rules of use; OA articles are governed by the applicable Creative Commons License

performed the experiments; and MC designed the experiments and wrote the article.

ORCID

Maurizio Chiurazzi https://orcid.org/0000-0003-2023-9572
Alessandra Rogato https://orcid.org/0000-0002-0373-9076
Stefano Sol https://orcid.org/0000-0003-2576-0156
Vladimir Totev Valkov https://orcid.org/0000-0002-3811-0913

References

Appleby CA. 1984. Leghemoglobin and *Rhizobium* respiration. *Annual Review Plant Physiology Plant Molecular Biology* **35**: 443–478.

Barbulova A, D'Apuzzo E, Rogato A, Chiurazzi M. 2005. Improved procedures for *in vitro* regeneration and for phenotypical analysis in the model legume *Lotus japonicus*. *Functional Plant Biology* **32**: 529–536.

Barbulova A, Rogato A, D'Apuzzo E, Omrane S, Chiurazzi M. 2007. Differential effects of combined N sources on early steps of the Nod factor-dependent transduction pathway in *Lotus japonicus*. *Molecular Plant–Microbe Interactions* **20**: 994–1003.

Bastianelli F, Costa A, Vescovi M, D'Apuzzo E, Zottini M, Chiurazzi M, Lo Schiavo F. 2009. Salicylic acid differentially affects suspension cell cultures of *Lotus japonicus* and one of its non-symbiotic mutants. *Plant Molecular Biology* **72**: 469–483.

Baudouin E, Pieuchot L, Engler G, Pauly N, Puppo A. 2006. Nitric oxide is formed in *Medicago truncatula–Sinorhizobium meliloti* functional nodules. *Molecular Plant–Microbe Interactions* **19**: 970–975.

Bergensen FJ. 1996. Delivery of O_2 to bacteroids. *Protoplasma* **191**: 9–20.

Bethke PC, Libourel IG, Jones RL. 2006. Nitric oxide reduces seed dormancy in *Arabidopsis*. *Journal of Experimental Botany* **57**: 517–526.

Bourcy M, Brocard L, Pislariu CI, Cosson V, Mergaert P, Tadege M, Mysore KS, Udvardi MK, Gourion B, Ratet P. 2013. *Medicago truncatula* DNF2 is a PI-PLC-XD-containing protein required for bacteroid persistence and prevention of nodule early senescence and defence-like reactions. *New Phytologist* **197**: 1250–1261.

Cabeza R, Koester B, Liese R, Lingner A, Baumgarten V, Dirks J, Salinas-Riester G, Pommerenke C, Dittert K, Schulze J. 2014. An RNA sequencing transcriptome analysis reveals novel insights into molecular aspects of the nitrate impact on the nodule activity of *Medicago truncatula*. *Plant Physiology* **164**: 400–411.

Cai C, Wang JY, Zhu YG, Shen QR, Li B, Tong YP, Li ZS. 2008. Gene structure and expression of the high-affinity nitrate transport system in rice roots. *Journal of Integrative Plant Biology* **50**: 443–451.

Cam Y, Pierre O, Boncompagni E, Herouart D, Meilhoc E, Bruand C. 2012. Nitric oxide (NO): a key player in the senescence of *Medicago truncatula* root nodules. *New Phytologist* **196**: 548–560.

Carroll B, Gresshoff PM. 1983. Nitrate inhibition of nodulation and nitrogen fixation in white clover. *Zeitschrift fur Pflanzenphysiologie* **110**: 69–76.

Chopin F, Orsel M, Dorbe MF, Chardon F, Truong HN, Miller AJ, Krapp A, Daniel-Vedele F. 2007. The *Arabidopsis* ATNRT2.7 nitrate transporter controls nitrate content in seeds. *Plant Cell* **19**: 1590–1602.

Clarke VC, Loughlin C, Gavrin A, Chen C, Brear EM, Day DA, Smith PMC. 2015. Proteomic analysis of the soybean symbiosome identifies new symbiotic proteins. *Molecular and Cellular Proteomics* **14**: 1301–1322.

Colebatch G, Desbrosses G, Ott T, Krusell L, Montanari O, Kloska S, Kopka J, Udvardi MK. 2004. Global changes in transcription orchestrate metabolic differentiation during symbiotic nitrogen fixation in *Lotus japonicus*. *The Plant Journal* **39**: 487–512.

Criscuolo G, Valkov VT, Parlati A, Martin-Alves L, Chiurazzi M. 2012. Molecular characterization of the *Lotus japonicus NRT1(PTR)* and *NRT2* families. *Plant, Cell & Environment* **35**: 1567–1581.

D'Apuzzo E, Valkov TV, Parlati A, Omrane S, Barbulova A, Sainz MM, Lentini M, Esposito S, Rogato A, Chiurazzi M. 2015. PII overexpression in *Lotus japonicus* affects nodule activity in permissive low nitrogen conditions and increases nodule numbers in high nitrogen treated plants. *Molecular Plant–Microbe Interactions* **28**: 432–442.

Earley KW, Haag JR, Pontes O, Opper K, Juehne T, Song K, Pikaard CS. 2006. Gateway-compatible vectors for plant functional genomics and proteomics. *The Plant Journal* **45**: 616–629.

Felsenstein J. 1985. Confidence limits on phylogenies: an approach using the bootstrap. *Evolution* **39**: 783–791.

Ferraioli S, Tatè R, Rogato A, Chiurazzi M, Patriarca JE. 2004. Development of Ectopic roots from abortive nodule primordia. *Molecular Plant–Microbe Interactions* **17**: 1043–1050.

Fu Y, Yi H, Bao J, Gong J. 2015. *LeNRT2.3* functions in nitrate acquisition and long-distance transport in tomato. *Federation of European Biochemical Societies Letters* **589**: 1072–1079.

Fujikake H, Yamazaki A, Ohtake N, Sueyoshi K, Matsuhashi S, Ito T, Mizuniwa C, Kume T, Hashimoto S, Ishioka NS. 2003. Quick and reversible inhibition of soybean root nodule growth by nitrate involves a decrease in sucrose supply to nodules. *Journal of Experimental Botany* **54**: 1379–1388.

Fukai E, Soyano T, Umehara Y, Nakayama S, Hirakawa H, Tabata S, Sato S, Hayashi M. 2012. Establishment of a *Lotus japonicus* gene tagging population using the exon-targeting endogenous retrotransposon LORE1. *The Plant Journal* **69**: 720–730.

Gamborg OL. 1970. The effects of amino acids and ammonium on the growth of plant cells in suspension culture. *Plant Physiology* **45**: 372–375.

Garcìa-Calderon M, Chiurazzi M, Espuny MR, Màrquez AJ. 2012. Photorespiratory metabolism and nodule function: behavior of *Lotus japonicus* mutants deficient in plastid glutamine synthetase. *Molecular Plant–Microbe Interactions* **25**: 211–219.

Gibbs J, Greenway H. 2003. Mechanisms of anoxia tolerance in plants. I. Growth, survival and anaerobic catabolism. *Functional Plant Biology* **30**: 1–47.

del Giudice J, Cam Y, Damiani I, Fung-Chat F, Meilhoc E, Bruand C, Brouquisse R, Puppo A, Boscari A. 2011. Nitric oxide is required for an optimal establishment of the *Medicago truncatula-Sinorhizobium meliloti* symbiosis. *New Phytologist* **191**: 405–417.

Glass ADM, Brito DT, Kaiser BN, Kronzucker HJ, Kumar A, Okamoto M, Rawat SR, Siddiqi MY, Silim SM, Vidmar JJ *et al.* 2001. Nitrogen transport in plants, with an emphasis on the regulation of fluxes to match plant demand. *Journal of Plant Nutrition Soil Science* **164**: 199–207.

Gu C, Song A, Zhang X, Wang H, Li T, Chen Y, Jiang J, Chen F, Chen S. 2016. Cloning of *Chrysanthenum* high-affinity nitrate transporter family (*CmNRT2*) and characterization of *CmNRT2.1*. *Science Reports* **6**: 23462.

Gutierrez RA, Stokes TL, Thum K, Xu X, Obertello M, Katari MS, Tanurdzic M, Dean A, Nero DC, McClung CR *et al.* 2008. Systems approach identifies an organic nitrogen-responsive gene network that is regulated by the master clock control gene *CCA1*. *Proceedings National Academic Science, USA* **105**: 4939–4944.

Handberg K, Stougaard J. 1992. *Lotus japonicus*, an autogamous, diploid legume species for classical and molecular genetics. *The Plant Journal* **2**: 487–496.

He X, Qu B, Li W, Zhao X, Teng W, Ma W, Ren Y, Li B, Li Z, Tong Y. 2015. The nitrate-inducible NAC transcription factor TaNAC2-5A controls nitrate response and increases wheat yield. *Plant Physiology* **169**: 1991–2005.

Hicri I, Boscari A, Castella C, Rovere M, Puppo A, Brouquisse R. 2015. Nitric oxide: a multifaceted regulator of the nitrogen-fixing symbiosis. *Journal of Experimental Botany* **66**: 2877–2887.

Ho CH, Lin SH, Hu HC, Tsay YF. 2009. *CHL1* functions as a nitrate sensor in plants. *Cell* **138**: 1184–1194.

Hogslund N, Radutoiu S, Krusell L, Voroshilova V, Hannah MA, Goffard N, Sanchez DH, Lippold F, Ott T, Sata S *et al.* 2009. Dissection of symbiosis and organ development by integrated transcriptome analysis of *Lotus japonicus* mutant and wild-type plants. *PLoS ONE* **4**: e6556.

Horchani F, Prévot M, Boscari A, Evangelisti E, Meilhoc E, Bruand C, Raymond M, Boncompagni E, Aschi-Smiti S, Puppo A *et al.* 2011. Both plant and bacterial nitrate reductases contribute to nitric oxide production in *Medicago truncatula* nitrogen-fixing nodules. *Plant Physiology* **155**: 1023–1036.

© 2020 The Authors
New Phytologist © 2020 New Phytologist Trust

14698137, 2020, 2, Downloaded from https://nph.onlinelibrary.wiley.com/doi/10.1111/nph.16728 by CNR GROUP II Istituto di Scienza dell', Wiley Online Library on [23/05/2024]. See the Terms and Conditions (https://onlinelibrary.wiley.com/terms-and-conditions) on Wiley Online Library for rules of use; OA articles are governed by the applicable Creative Commons License

14698137, 2020, 2, Downloaded from https://nph.onlinelibrary.wiley.com/doi/10.1111/nph.16728 by CNR GROUP II Istituto di Scienza dell', Wiley Online Library on [23/05/2024]. See the Terms and Conditions (https://onlinelibrary.wiley.com/terms-and-conditions) on Wiley Online Library for rules of use; OA articles are governed by the applicable Creative Commons License

Hussain AK, Jiang Q, Broughton WJ, Gresshoff PM. 1999. *Lotus japonicus* nodulates and fixes nitrogen with the broad host range *Rhizobium* sp. NGR234. *Plant Cell Physiology* **40**: 894–899.

Ibrahim A, Jin XL, Zhang YB, Cruz J, Vichyavichien P, Esiobu N, Zhang XH. 2017. Tobacco plants expressing the maize nitrate transporter *ZmNrt2.1* exhibit altered responses of growth and gene expression to nitrate and calcium. *Botanical Studies* **58**: 51.

Jefferson RA. 1987. Assaying chimeric genes in plants: the *GUS* gene fusion system. *Plant Molecular Biology Reports* **5**: 387–405.

Jeudy C, Ruffell S, Freixes S, Tillard P, Santoni AL, Morel S, Journet EP, Duc G, Gojon A, Lepetit M *et al.* 2010. Adaptation of *Medicago truncatula* to nitrogen limitation is modulated via local and systemic nodule developmental responses. *New Phytologist* **85**: 817–828.

Jiang Q, Gresshoff PM. 1997. Classical and molecular genetics of the model legume *Lotus japonicus*. *Molecular Plant–Microbe Interactions* **10**: 59–68.

Jones DT, Taylor WR, Thornton JM. 1992. The rapid generation of mutation data matrices from protein sequences. *Computer Applications in the Biosciences* **8**: 275–282.

Kato K, Kanahama K, Kanayama Y. 2010. Involvement of nitric oxide in the inhibition of nitrogenase activity by nitrate in *Lotus* root nodules. *Journal of Plant Physiology* **167**: 238–241.

Kiba T, Feria-Bourrellier AB, Lafouge F, Lezhneva L, Boutet-Mercey S, Orsel M, Brèhaut V, Miller A, Daniel-vedele F, Sakakibara H *et al.* 2012. The *Arabidopsis* nitrate transporter *NRT2.4* plays a double role in roots and shoots of nitrogen-starved plants. *Plant Cell* **24**: 245–258.

Kotur Z, Mackenzie N, Ramesh S, Tyerman SD, Kaiser BN, Glass AD. 2012. Nitrate transport capacity of the *Arabidopsis thaliana* NRT2 family members and their interactions with AtNAR2.1. *New Phytologist* **194**: 724–731.

Krussell L, Krause K, Ott T, Desbrosses G, Kramer U, Sato S, Nakamura Y, Tabata S, James EK, Sandal N *et al.* 2005. The sulfate transporter *SST1* is crucial for symbiotic nitrogen fixation in *Lotus japonicus* root nodules. *Plant Cell* **17**: 1625–1636.

Kumar S, Stecher G, Tamura K. 2016. MEGA 7: Molecular Evolutionary Genetics Analysis version 7.0 for bigger datasets. *Molecular Biology and Evolution* **33**: 1870–1874.

Leblanc A, Segura R, Deleu C, Le Deunff E. 2013. In low transpiring conditions, uncoupling the *BnNrt2.1* and *BnNRT1.1* NO_3^- transporters by glutamate treatment reveals the essential role of *BnNRT2.1* for nitrate uptake and the nitrate-signaling cascade during growth. *Plant Signaling & Behavior* **8**: e22904.

Léran S, Varala K, Boyer JC, Chiurazzi M, Crawford N, Daniel-Vedele F, David L, Dickstein R, Fernandez E, Forde B *et al.* 2014. A unified nomenclature of Nitrate Transporter 1/Peptide Transporter family members in plants. *Trends in Plant Science* **19**: 5–9.

Lezhneva L, Kiba T, Feria-Bourrellier AB, Lafouge F, Boutet-Mercey S, Zoufan P, Sakakibara H, Daniele-vedele F, Krapp A. 2014. The *Arabidopsis* nitrate transporter *NRT2.5* plays a role in nitrate acquisition and remobilization in nitrogen-starved plants. *The Plant Journal* **80**: 230–241.

Li Y, Li J, Yan Y, Liu W, Zhang W, Gao L, Tian Y. 2018. Knock down of CsNRT2.1, a cucumber nitrate transporter, reduces nitrate uptake, root length, and lateral root number at low external nitrate concentration. *Frontiers in Plant Science* **9**: 722.

Lin JS, Li X, Luo Z, Mysore KS, Wen J, Xie F. 2018. NIN interacts with NLPs to mediate nitrate inhibition of nodulation in *Medicago truncatula*. *Nature Plants* **4**: 942–952.

Luo B, Xu M, Zhao L, Xie P, Chn Y, Harwood W, Xu G, Fan X, Miller AJ. 2020. Overexpression of the high-affinity nitrate transporter *OsNRT2.3b* driven by different promoters in barley improves yield and nutrient uptake balance. *International Journal of Molecular Sciences* **15**: 21.

Malolepszy A, Mun T, Sandal N, Gupta V, Dubin M, Urbański DF, Shan N, Bachmann A, Fukai E, Hirakawa H *et al.* 2016. The LORE1 insertion mutant resource. *The Plant Journal* **88**: 306–317.

Meakin GE, Bueno E, Jepson B, Bedmar EJ, Richardson DJ, Delgado MJ. 2007. The contribution of bacteroidal nitrate and nitrite reduction to the formation of nitrosylleghaemoglobin complexes in soybean root nodules. *Microbiology* **153**: 411–419.

Meilhoc E, Cam Y, Skapski A, Bruand C. 2010. The response to nitric oxide of the nitrogen-fixing symbiont *Sinorhizobium meliloti*. *Molecular Plant–Microbe Interactions* **23**: 748–759.

Minchin FR, Minguez MI, Sheehy JE, Witty JF, Skøt L. 1986. Relationships between nitrate and oxygen supply in symbiotic nitrogen fixation by white clover. *Journal of Experimental Botany* **37**: 1103–1113.

Nagata M, Murakami E, Shimoda Y, Shimoda-Sasakura F, Kucho K, Suzuki A, Abe M, Higashi S, Uchiumi T. 2008. Expression of a class 1 *hemoglobin* gene and production of nitric oxide in response to symbiotic and pathogenic bacteria in *Lotus japonicus*. *Molecular Plant–Microbe Interactions* **21**: 1175–1183.

Naudin C, Corre-Hellou G, Voisin AS, Oury V, Salon C, Crozat Y, Jeuffroy MH. 2011. Inhibition and recovery of symbiotic N_2 fixation by peas (*Pisum sativum* L.) in response to short-term nitrate exposure. *Plant and Soil* **346**: 275–287.

Naz M, Luo B, Guo X, Li B, Chen J, Fan X. 2019. Overexpression of nitrate transporter *OsNRT2.1* enhances nitrate-dependent root elongation. *Genes* **9**: 10.

Nishida H, Tanaka S, Handa Y, Ito M, Sakamoto Y, Matsunaga S, Betsuyaku S, Miura K, Soyano T, Kawaguchi M *et al.* 2018. A NIN-LIKE PROTEIN mediates nitrate-induced control of root nodule symbiosis in *Lotus japonicus*. *Nature Communications* **9**: 499.

Omrane S, Chiurazzi M. 2009. A variety of regulatory mechanisms are involved in the nitrogen-dependent modulation of the nodule organogenesis program in legume roots. *Plant Signaling and Behaviour* **4**: 1066–1068.

Omrane S, Ferrarini A, D'Apuzzo E, Rogato A, Delledonne M, Chiurazzi M. 2009. Symbiotic competence in *Lotus japonicus* is affected by plant nitrogen status: transcriptomic identification of genes affected by a new signalling pathway. *New Phytologist* **183**: 380–394.

Ott T, van Dongen JT, Gunther C, Krussell L, Desbrosses G, Vigeolas H, Bock V, Czechowski T, Geigenberger P, Udvardi MK. 2005. Symbiotic leghemoglobins are crucial for nitrogen fixation in legume root nodules but not for general plant growth and development. *Current Biology* **15**: 531–535.

Pajuelo P, Pajuelo E, Orea A, Romero JM, Marquez AJ. 2002. Influence of plant age and growth conditions on nitrate assimilation in roots of *Lotus japonicus* plants. *Functional Plant Biology* **29**: 485–494.

Pedrazzini E, Giovinazzo G, Bielli A, de Virgilio M, Frigerio L, Pesca M, Faoro F, Bollini R, Ceriotti A, Vitale A. 1997. Protein quality control along the route to the plant vacuole. *Plant Cell* **9**: 1869–1880.

Pellizzaro A, Clochard T, Planchet E, Limami AM, Morère-Le Paven MC. 2015. Identification and molecular characterization of *Medicago truncatula* NRT2 and NAR2 families. *Physiologia Plantarum* **154**: 256–269.

Pislariu CI, Murray JD, Wen JQ, Cosson V, Muni RRD, Wang M, Benedito VA, Andriankaja A, Cheng X, Jerez IT *et al.* 2012. A *Medicago truncatula* tobacco retrotransposon insertion mutant collection with defects in nodule development and symbiotic nitrogen fixation. *Plant Physiology* **159**: 1686–1699.

Plett D, Toubia J, Garnett T, Tester M, Kaiser BN, Baumann U. 2010. Dichotomy in the *NRT* gene families of dicots and grass species. *PLoS ONE* **5**: e15289.

Puppo A, Groten K, Bastian F, Carzaniga R, Soussi M, Lucas MM, de Felipe MR, Harrison J, Vanacker H, Foyer CH. 2005. Legume nodule senescence: roles for redox and hormone signalling in the orchestration of the natural aging process. *New Phytologist* **165**: 683–701.

Rogato A, D'Apuzzo E, Barbulova A, Omrane S, Stedel K, Simon-Rosin U, Katinakis P, Flemetakis M, Udvardi M, Chiurazzi M. 2008. Tissue-specific down-regulation of *LjAMT1;1* compromises nodule function and enhances nodulation in *Lotus japonicus*. *Plant Molecular Biology* **68**: 585–595.

Rogato A, D'Apuzzo E, Chiurazzi M. 2010. The multiple plant response to high ammonium conditions. The *Lotus japonicus* AMT1;3 protein acts as a putative transceptor. *Plant Signaling and Behavior* **5**: 1584–1586.

Rogato A, Valkov TV, Alves LM, Apone F, Colucci G, Chiurazzi M. 2016. Down-regulated *Lotus japonicus GCR1* plants exhibit nodulation signalling pathways alteration. *Plant Science* **247**: 71–82.

Saitou N, Nei M. 1987. The neighbor-joining method: a new method for reconstructing phylogenetic trees. *Molecular Biology and Evolution* **4**: 406–425.

Sanchez C, Gates AJ, Meakin GE, Uchiumi T, Girard L, Richardson DJ, Bedmar EJ, Delgado MJ. 2010. Production of nitric oxide and nitrosylleghemoglobin complexes in soybean nodules in response to flooding. *Molecular Plant–Microbe Interactions* **23**: 702–711.

© 2020 The Authors
New Phytologist © 2020 New Phytologist Trust

Santi C, von Groll U, Ribeiro A, Chiurazzi M, Auguy F, Bogusz D, Franche C, Pawlowski K. 2003. Comparison of nodule induction in legume and actinorhizal symbioses: the induction of actinorhizal nodules does not involve *ENOD40*. *Molecular Plant–Microbe Interactions* **16**: 808–816.

Schulze J, Liese R, Ballesteros G, Casieri L, Salinas G, Cabeza RA. 2020. Ammonium acts systemically while nitrate exerts an additional local effect on *Medicago truncatula* nodules. *Plant Science* **292**: 110383.

Shimoda Y, Shimoda-Sasakura F, Kucho K, Kanamori N, Nagata M, Suzuki A, Abe M, Higashi S, Uchiumi T. 2009. Overexpression of class 1 plant *hemoglobin* genes enhances symbiotic nitrogen fixation activity between *Mesorhizobium loti* and *Lotus japonicus*. *The Plant Journal* **57**: 254–263.

Sol S, Valkov TV, Rogato A, Noguero M, Gargiulo L, Mele G, Lacombe B, Chiurazzi M. 2019. Disruption of the *Lotus japonicus* transporter LjNPF2.9 increases shoot biomass and nitrate content without affecting symbiotic performances. *BMC Plant Biology* **19**: 380.

Stougaard J, Abildsten D, Marcker KA. 1987. The *Agrobacterium rhizogenes* pRi TL-DNA segment as a gene vector system for transformation of plants. *Molecular General Genetics* **207**: 251–255.

Swift J, Adame M, Tranchina D, Henry A, Coruzzi GM. 2019. Water impacts nutrient dose responses genome-wide to affect crop production. *Nature Communications* **10**: 1374.

Takanashi K, Takanashi H, Sakurai N, Sugiyama A, Suzuki H, Shibata D, Nakazono M, Yazaki K. 2012. Tissue-specific transcriptome analysis in nodules of *Lotus japonicus*. *Molecular Plant–Microbe Interactions* **25**: 869–876.

Tang Z, Fan X, Li Q, Feng H, Miller AJ, Shen Q, Xu G. 2012. Knockdown of a rice stelar nitrate transporter alters long-distance translocation but not root influx1. *Plant Physiology* **160**: 2052–2063.

Taulemesse F, Le Gouis J, Gouache D, Gibon Y, Allard V. 2015. Post-flowering nitrate uptake in wheat is controlled by N status at flowering, with a putative major role of root nitrate transporter NRT2.1. *PLoS ONE* **23**: 10.

Teillet A, Garcia J, de Billy F, Gherardi M, Huguet T, Barker DG, de Carvalho-Niebel F, Journet EP. 2008. Api, a novel *Medicago truncatula* symbiotic mutant impaired in nodule primordium invasion. *Molecular Plant–Microbe Interactions* **21**: 535–546.

Trinchant JC, Rigaud J. 1982. Nitrite and nitric oxide as inhibitors of nitrogenase from soybean bacteroids. *Applied and Environmental Microbiology* **44**: 1385–1388.

Tsay YF, Chiu CC, Tsai CB, Ho CH, Hsu PK. 2007. Nitrate transporters and peptide transporters. *Federation of European Biochemical Societies Letters* **581**: 2290–300.

Tusnády GE, Simon I. 2001. The HMMTOP transmembrane topology prediction server. *Bioinformatics* **17**: 849–850.

Urbanski DF, Małolepszy A, Stougaard J, Andersen SU. 2012. Genome-wide LORE1 retrotransposon mutagenesis and high-throughput insertion detection in *Lotus japonicus*. *The Plant Journal* **69**: 731–741.

Valkov TV, Chiurazzi M. 2014. Nitrate transport and signaling. In: Tabata S, Stougaard J, eds. *The* Lotus japonicus *genome, compendium of plant genomes*. Berlin, Germany: Springer, 125–136.

Valkov TV, Rogato A, Alves LM, Sol S, Noguero M, Léran S, Lacombe B, Chiurazzi M. 2017. The Nitrate Transporter Family Protein LjNPF8.6 controls the N-fixing nodule activity. *Plant Physiology* **175**: 1269–1282.

Vance CP. 2008. Carbon and nitrogen metabolism in legume nodules. In: Dilworth MJ, James EK, Sprent JI, Newton WE, eds. *Nitrogen-fixing leguminous symbioses*. Dordrecht, the Netherlands: Kluwer Academic, 293–320.

Verdier J, Torres-Jerez I, Wang M, Andriankaja A, Allen SN, He J, Tang Y, Murray JD, Udvardi MK. 2013. Establishment of the *Lotus japonicus* gene expression atlas (LjGEA) and its use to explore legume seed maturation. *The Plant Journal* **74**: 351–362.

Vessey JK, Walsh KB, Layzell DB. 1988. Oxygen limitation of N_2 fixation in stem-girdled and nitrate-treated soybean. *Physiologia Plantarum* **73**: 113–121.

Vessey JK, Waterer J. 1992. In search of the mechanism of nitrate inhibition of nitrogenase activity in legume nodules: recent developments. *Physiologia Plantarum* **84**: 171–176.

Wang J, Huner N, Tian L. 2019. Identification and molecular characterization of the *Brachypodium distachyon NRT2* family, with a major role of BdNRT2.1. *Physiologia Plantarum* **165**: 498–510.

Wang YY, Cheng YH, Chen YE, Tsay WF. 2018. Nitrate transport, signaling, and use efficiency. *Annual Review of Plant Biology* **69**: 27.1–27.38.

Wei J, Zheng Y, Feng H, Qu H, Fan X, Yamaji N, Ma JF, Xu G. 2018. *OsNRT2.4* encodes a dual-affinity nitrate transporter and functions in nitrate-regulated root growth and nitrate distribution in rice. *Journal of Experimental Botany* **69**: 1095–1107.

Witty JF, Minchin FR. 1998. Hydrogen measurements provide direct evidence for a variable physical barrier to gas diffusion in legume nodules. *Journal of Experimental Botany* **49**: 1015–1020.

Yendrek CR, Lee YC, Morris V, Liang Y, Pislariu CI, Burkart G, Meckfessel H, Salehin M, Kessler H, Wessler H *et al.* 2010. Putative transporter is essential for integrating nutrient and hormone signaling with lateral root growth and nodule development in *Medicago truncatula*. *The Plant Journal* **62**: 100–112.

Zou L, Qi D, Sun J, Zheng X, Peng M. 2019. Expression of the cassava nitrate transporter *NRT2.1* enables *Arabidopsis* low nitrate tolerance. *Journal of Genetics* **98**: 74.

Zou X, Liu MY, Wu WH, Wang Y. 2019. Phosphorylation at Ser28 stabilizes the *Arabidopsis* nitrate transporter *NRT2.1* in response to nitrate limitation. *Journal of Integrative Plant Biology* **62**: 865–876.

Supporting Information

Additional Supporting Information may be found online in the Supporting Information section at the end of the article.

Fig. S1 Amino acid sequence of *L. japonicus* NRT2.4 protein.

Fig. S2 Phenotypic symbiotic characterization of the *Ljnrt2.4* nodules.

Fig. S3 Phenotypic characterization of the *L. japonicus Ljnrt2.4-1* and *Ljnrt2.4-2* plants.

Table S1 Nomenclature of the complete list of *L. japonicus NRT2* genes and values of amino acid identity between LjNRT2.4 and AtNRT2 members.

Table S2 Oligonucleotides used in the present work.

Please note: Wiley Blackwell are not responsible for the content or functionality of any Supporting Information supplied by the authors. Any queries (other than missing material) should be directed to the *New Phytologist* Central Office.

© 2020 The Authors
New Phytologist © 2020 New Phytologist Trust

14698137, 2020, 2, Downloaded from https://nph.onlinelibrary.wiley.com/doi/10.1111/nph.16728 by CNR GROUP II Istituto di Scienza dell', Wiley Online Library on [23/05/2024]. See the Terms and Conditions (https://onlinelibrary.wiley.com/terms-and-conditions) on Wiley Online Library for rules of use; OA articles are governed by the applicable Creative Commons License